Thermomagnetic and thermoelectric properties of potassium

M. R. Stinson and R. Fletcher
Physics Department, Queen's University, Kingston, Ontario K7L 3N6, Canada

C. R. Leavens
Division of Physics, National Research Council, Ottawa, Ontario K1A 0R6, Canada

(Received 14 May 1979)

We present the results of an experimental and theoretical study of the thermal and thermoelectric properties of pure potassium for zero magnetic field and for fields up to 4.5 T, at temperatures of 1.5–4.2 K. The approximate quadratic dependence on field of the transverse thermal magnetoresistivity is found to be the result of a high lattice conductivity. It is shown that phonon-electron scattering cannot be completely responsible for limiting the lattice conductivity and it is suggested that phonon-dislocation scattering plays an essential role at low temperatures. High-field semiclassical theory completely accounts for the observed field variations of the thermal magnetoresistivities (both transverse and Righi-Leduc) once the presence of the large lattice thermal conductivity is accepted. The study of the high-field Nernst-Ettingshausen coefficient has augmented the information gained from the lattice thermal conductivity. The analysis of this coefficient shows unambiguously that (i) the phonon-drag contribution plays a central role, (ii) the phonon drag is significantly quenched pointing to at least one additional important scattering process for phonons other than phonon-electron, (iii) the strength of the additional scattering required to limit the lattice conductivity to the experimental values provides the observed quenching, (iv) phonon-electron umklapp processes begin to become significant at about 2 K. Experimental results and their analysis are also presented on the thermopower of potassium, a property which provides similar information to the Nernst-Ettingshausen coefficient but not unambiguously.

I. INTRODUCTION

The present work was undertaken as part of a systematic investigation of the magnetotransport properties of potassium. There are many published papers on the electrical magnetoresistivities (that is, the transverse and longitudinal magnetoresistivities and the Hall resistivity), but relatively few on the thermal and thermoelectric properties; for this reason we have concentrated on these latter. In this Introduction we shall attempt to summarize the present experimental and theoretical situation with regard to the thermal and thermoelectric coefficients; we begin with the former.

A few years ago, it was shown that an estimate of the lattice thermal conductivity of uncompensated pure metals could be obtained from their magnetothermal resistivities.[1,2] The principle is very simple and we shall outline it since it has a bearing on our present measurements and discussion. As usual, let us define the transport tensors according to

$$\vec{J} = \vec{\sigma}\vec{E} + \vec{\epsilon}''\vec{\nabla}T, \tag{1a}$$

$$\vec{U} = -\vec{\pi}''\vec{E} - \vec{\lambda}''\vec{\nabla}T, \tag{1b}$$

where $\vec{J}$ and $\vec{U}$ represent the electrical and thermal current densities, $\vec{E}$ is the electric field, $\vec{\nabla}T$ the temperature gradient, and $\vec{\sigma}$, $\vec{\epsilon}''$, $\vec{\pi}''$ and $\vec{\lambda}''$ are the various transport tensors. Let us restrict the outline to a cubic metal with a simple Fermi surface that does not intersect the zone boundaries (typified by potassium[3]). We assume that the total thermal conductivity $\vec{\lambda}''$ is a linear sum of that due to the electrons $\vec{\lambda}^e$ and that due to the lattice $\vec{\lambda}^g$.

If the crystal is cubic, $\vec{\lambda}^g$ is simply a scalar whatever the direction of the magnetic field B (i.e., the tensor is diagonal and all nonzero components have the same value λ^g). We further assume that $\vec{\lambda}^e$ takes the simple form

$$\vec{\lambda}^e = \begin{bmatrix} \lambda^e_{xx} & \lambda^e_{xy} & 0 \\ -\lambda^e_{xy} & \lambda^e_{xx} & 0 \\ 0 & 0 & \lambda^e_{zz} \end{bmatrix},$$

which would certainly be true if $\vec{B}$ were along a crystal axis of high symmetry (threefold or more) or if the sample was a polycrystal with small crystallites; however, for such a simple metal as potassium, we expect that $\vec{\lambda}^e$ would not be sensitive to the direction of $\vec{B}$ relative to the crystal axes. (Throughout this paper, we shall assume that all the tensors have such a form.)

At high B (i.e., $\omega\tau \gg 1$, which typically means $B \gtrsim 0.1$ T for reasonably good samples of K), it has been shown[4] that the components of $\vec{\lambda}^e$ should take the limiting form

$$\lambda^e_{xx} = \alpha(T)/B^2 \ , \tag{2a}$$

$$\lambda^e_{xy} = L_0 Tne/B \ , \tag{2b}$$

where $\alpha(T)$ is a function of T but not B, L_0 is the Sommerfeld value of the Lorenz number, T the temperature, n the number of electrons per unit volume, and e the electronic charge. The measured quantities are, in fact, the components of the thermal resistivity tensor $\vec{\gamma}$, which to high accuracy are obtained from $\vec{\gamma} = \vec{\lambda}''^{-1}$. Thus the thermal magnetoresistivity is given by

$$\gamma_{xx} = \frac{\alpha(T)/B^2 + \lambda^g}{[\alpha(T)/B^2 + \lambda^g]^2 + (L_0 Tne/B)^2} \ . \tag{3}$$

It seems to be true in general that there is a range of B for which

$$(L_0 Tn|e|/B)^2 \gg (\alpha/B^2 + \lambda^g)^2 \ ,$$

i.e., not too high a field that $\lambda^g \sim L_0 Tn|e|/B$, but high enough so that $\omega\tau \gg 1$ is satisfied. In this range it is a good approximation to write

$$\gamma_{xx} = \alpha(T)/(L_0 Tne)^2 + \lambda^g (B/L_0 Tne)^2 \ .$$

The first term depends only on T and corresponds to the (field-independent) resistivity when $\lambda^g = 0$, and the second term, which is quadratic in B, yields λ^g. The principle was applied to K and λ^g was deduced.[1] However the λ^g so obtained had a much higher magnitude than theoretically predicted, and also had an unusual temperature dependence. Other independent data[5,6] on γ_{xx} were in good agreement but the explanation of the B^2 component in terms of λ^g was received with skepticism in view of the unexpected behavior of the derived λ^g.

More recently, Tausch and Newrock[7] extended the measurement of the thermal magnetoresistivities of K to very high fields. Their results showed that γ_{xx} increases as B^2 at least up to fields of 9–10 T, whereas Eq. (3) suggests that deviations from B^2 should become appreciable when $\lambda^g \sim L_0 Tn|e|/B$; the early data[1] on λ^g indicate that this equality is satisfied in the region of 10 T. Tausch and Newrock[7] concluded that a large fraction of the B^2 term in γ_{xx} must originate in some way other than through λ^g as outlined here, but gave no specific suggestions. Nevertheless they attempted to obtain λ^g from their results and deduced values smaller by a factor of about 15 than those obtained earlier. However it has been shown[8] that if one evaluates $\lambda^e_{xy} = \gamma_{yx}/(\gamma^2_{yx} + \gamma^2_{xx})$ from their data, then the value obtained is about 50% smaller than $L_0 Tn|e|/B$ by 9 T. This disagreement with the high-field semiclassical prediction of the Lifshitz-Azbel'-Kaganov (LAK) theory[4] is by far the worse ever reported for an off-diagonal term. Data on other uncompensated metals (Al and In) show no such discrepancies,[9] though it is true that the available fields were much lower in those experiments.

In view of the unexpected results of Tausch and Newrock,[7] and the generally unsatisfactory situation as regards the influence of λ^g on the thermomagnetic coefficients, we decided to remeasure the thermal resistivities of potassium to high fields; this paper presents our new results. Although our maximum field (~4.5 T) is lower than that of Tausch and Newrock (~ 9 T), we see that their results already indicate a reduction of $|\lambda^e_{xy}|$ of 15–20% below the theoretical value by this field.

We shall show, contrary to the results of Tausch and Newrock, that the anomalous thermomagnetic behavior of potassium, in particular, the approximate B^2 dependence of γ_{xx}, can be completely understood in terms of the effects of λ^g, and further that λ^e_{xy} has (within the 2% experimental error) the predicted value up to 4.5 T, our highest field. The values of λ^g that we obtain are in good agreement with the earlier experimental estimates,[1] but are still much higher than theory had led us to expect.[10] We believe that this large value of λ^g arises from a relatively small fraction of the phonons, those almost purely transverse phonons with (sufficiently small) wave vectors near the symmetry planes which are scattered only very weakly by the nearly-free electrons in potassium.

In addition to the above results, we believed that it would be equally important to investigate the thermoelectric properties of potassium. In the last few years, the study of the adiabatic Nernst-Ettingshausen coefficient P^a has proved very rewarding; this coefficient yields the off-diagonal thermoelectric component ϵ''_{yx}. The most interesting feature about ϵ''_{yx} is that, in the high-field limit, the diffusion component, say ϵ^d_{yx}, becomes independent of electronic scattering and has the limiting value[11]

$$\epsilon^d_{yx} = \pi^2 k_B^2 T N(\mu)/3B = \gamma T/B \ , \tag{4}$$

where k_B is Boltzmann's constant, $N(\mu)$ the electronic density of states at the chemical potential μ, and γT the low-temperature electronic specific heat. It has been shown[12] that $N(\mu)$ is exactly the same as that occurring in the electronic specific heat and is hence available, in the literature, to high accuracy. This means that any measured difference between the measured value ϵ''_{yx} and $\gamma T/B$ must be due to phonon drag, say ϵ^g_{yx}.

The coefficient ϵ''_{yx} has been investigated for other metals, but potassium should be a most in-

teresting case in that the normal and umklapp electron—phonon scattering processes can be clearly distinguished for such a simple Fermi surface; in this case the two types of scattering give rise to contributions to ϵ^{g}_{yx} of opposite signs. Thus a study of ϵ^{g}_{yx} can be used to positively identify the onset of the umklapp processes. A similar result could, in principle, be achieved from a study of the zero-field thermopower, but in this case there are possibly added complications due to higher-order scattering effects[13, 14] contributing to the diffusion term; thus there remains some doubt concerning the precise separation of the phonon drag from the diffusion term. It should be clearly understood that ϵ''_{yx} contains no such contributions in the high-field limit (i.e., the limit that we are considering here).

The clear separation of ϵ^{g}_{yx} allows one to provide a definitive test of the current theory of phonon drag. We shall show that theory and experiment are in very good agreement for potassium. We then show that the zero-field thermopower can be understood as arising from a calculable phonon-drag contribution and an additive contribution linear in T (this latter, however, is difficult to calculate and cannot be obtained from an independent experiment).

We have presented some preliminary findings on the thermal magnetoresistivities for one of the samples,[8] and given a much abbreviated outline of the comparison between the calculated and experimental results in the case of the λ^{g} and ϵ''_{yx}.[15]

The paper proceeds in Sec. II with an outline of our experimental techniques. This is followed by the presentation of the results (Sec. III) and the preliminary analysis required to obtain the quantities of interest. Section IV deals with our theoretical approach and Sec. V is devoted to a comparison of the experimental and theoretical results. Finally in Sec. VI we summarize our findings.

II. EXPERIMENTAL TECHNIQUES

Results were obtained on three polycrystalline samples of potassium (labeled samples 1–3). All preparation and mounting was carried out under cleaned argon in a glove box. The samples were cast into molds made from polyethylene and polypropylene using potassium obtained from the MSA Corporation.[16] After casting, samples 1 and 2 were slow cooled by leaving the molds at room temperature, but sample 3 was fast cooled by dipping one end of the mold in liquid nitrogen. The crystallites were never visible, even after storing under oil, so we are unable to give an estimate of their size. The samples were bent to the shape shown in Fig. 1 and mounted in a frame similar to that used previously,[17] but adapted for use in a superconducting solenoid rather than an electromagnet. Small copper blocks holding the carbon thermometers and potential leads were clamped to the limbs by means of plates and screws. The blocks were supported by the nylon rods, which were an integral part of the sample holder.[17] The vacuum can containing the sample had an inner diameter of 51 mm, allowing us to use relatively long samples, the distance between the bends being 38 mm. The samples were 5 mm wide, 1.5 mm thick, and the distance between the outermost pair of limbs was 19 mm. The width of the limbs was about 1.3 mm.

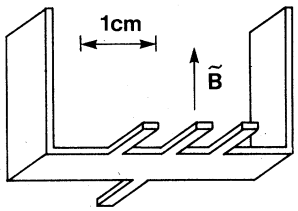

FIG. 1. Form of the samples when mounted in the cryostat. Scale is approximate.

By using limbs we are attempting to accurately control the geometry of the probes (the probes being the limbs plus the thermometers and potential wires) and avoid irreproducible effects caused by the probes interfering with the current distribution. There will be an error in assuming that the length-to-area ratio (required to evaluate the transverse electrical and thermal resistivities ρ_{xx} and γ_{xx}) is that appropriate to the body of the sample, i.e., ignoring the limbs. We have made an experimental estimate of this error by taking a brass sample (actually the original template for the mold) and measuring its resistance with and without the center limbs. We find that the resistance rises $(0.75 \pm 0.2)\%$ when the limbs are removed. We realize that the correction in high magnetic fields (where $|\sigma_{xy}| \gg \sigma_{xx}$) may not be exactly the same, but we assume it is similar. The presence of the limbs is irrelevant to the data reduction on the Hall and Righi-Leduc resistivities; i.e., only an accurate measure of the sample thickness is required.

We have investigated the possibility that "end effects" significantly influence our results,[18] and conclude that they do not (Appendix).

The sample mounting was carried out inside the glove box as was the sealing and evacuating of the sample vacuum can. The assembly was then transferred to the cryostat and allowed to stand at room temperature for about 24 h under high vacuum to anneal out any strains in the potassium caused by mounting. It was then cooled to liquid-nitrogen temperatures over a period of many hours

and subsequently to liquid-helium temperatures. In the case of samples 1 and 2, the cryostat was never allowed to warm significantly above 77 K thoughout the whole series of runs. The last sample had to be warmed to room temperature twice to correct superfluid-^{4}He leaks; this led to slight changes in some of the experimental quantities and these will be discussed further in Sec. III.

The thermometers were $\frac{1}{10}$-W 220-Ω Allen Bradley carbon resistors. They were calibrated against temperature using ^{4}He vapor pressure during every run[19] and the experimental data were corrected for their magnetic field dependence. We expect temperatures to be accurate to 0.1% and temperature differences to 0.6%. The power levels in each resistor were about 10 nW at 4 K, dropping to 2 nW at 1.5 K. The vapor pressure of the ^{4}He bath was stabilized using an electronic regulator,[20] the temperature being maintained to an accuracy of better than 1 mK.

The major experimental difficulty was in the measurement of the small Nernst-Ettingshausen potential differences (~ 1–15 nV). We made use of the superconducting chopper amplifier developed by Edwards.[21] Initially the choppers were enclosed in a capillary tube using vacuum grease, as in the originals, but after prolonged use these developed excessive noise and drift. For the last sample we used a chopper embedded in Stycast[22] 2850 FT; this did not show any degradation in time and was far more robust. Although the choppers had a zero-field resolution of about 10^{-11} V (with a 1-sec rise time), the unavoidable loops formed by the sample and potential leads, combined with residual vibrations and field fluctuations, led to induced emf's of the order of a few nV at high magnetic fields. We reduced this problem by stabilizing the gain of the amplifier[23] at an accurately known value (~ 0.1%) by the use of heavy negative feedback and averaging its output for times of 60–100 sec. The residual noise was rather variable from run to run and ranged from 10^{-10} V to perhaps an order of magnitude worse than this.

The magnetic field was produced by a solenoid which has no observable hysteresis (< 0.1%) above 0.5 T. The coil factor (i.e., the ratio of field to current) is known to an accuracy of ≤ 0.5%.

All the sample dimensions are corrected for thermal expansion.[24] It is worth pointing out that, although the sample and sample holder are matched for their thermal length contractions between room temperature and 4 K, it is unlikely that they are accurately matched at all intermediate temperatures. Thus it seems inevitable that some straining of the sample takes place during each cooldown and warmup.

III. RESULTS AND ANALYSIS

As we have already mentioned, the main aim of this work was to investigate the thermomagnetic and thermoelectric coefficients of K. For reasons that will become clear as we proceed, we have also obtained a somewhat limited amount of data on the transverse electrical resistivity ρ_{xx} and the Hall resistivity ρ_{yx}. These data are taken under adiabatic conditions but it will be an excellent approximation[2] to write $\vec{\rho} = \vec{\sigma}^{-1}$; this approximation is equivalent to that of $\vec{\gamma} = \vec{\lambda}''^{-1}$.

The results are most useful when available as complete sets for particular samples; we were able to obtain such sets for samples 2 and 3. The data on sample 1 are incomplete in that we were unable to obtain accurate results on ρ_{xx} (though this is not essential to our analysis) and we have no data whatever on the thermopower. We have limited our investigation to three samples because of the extensive time required to complete these measurements. It should be mentioned that samples 1 and 2 were made from the same batch of potassium, while sample 3 originated from a different batch.

It is useful at this point to say a few words about the sources of error in the coefficients we obtain, although we shall discuss each case as it arises in the subsequent presentation. As usual, the main source of error in many of the derived quantities is the measurement of the sample dimensions. We estimate, mainly from our previous experience with potassium, that there will probably be errors in the thickness of about 2%. The length should be accurate to 0.5%, but the width is known only to about 1%, mainly because of slight irregularities from a perfect rectangular shape. Generally speaking, these form factors will not affect the field or temperature variation of the primary measured quantities and the data can be internally consistent to much better than that quoted. Such is the case for γ_{xx} and γ_{yx}, which have total errors (including those in T and ΔT referred to earlier) of perhaps 4% and $2\frac{1}{2}$%, respectively, but for a single sample the scatter of the data will only reflect the thermometer calibrations and will be typically ~ 0.5% for each.

On the other hand, the derived quantities, for example those obtained by inverting $\vec{\gamma}$, depend on the dimensions in a way that is a function of field and temperature; this can lead to systematic errors in λ_{xx} and λ_{xy} of 0.4%, as the field is varied from its minimum to maximum value. It is clear that the details are more conveniently discussed at the same time as the data are presented.

The residual resistivity ratios ρ_{295}/ρ_0 for samples 1–3 are 6200, 4400, and 6400; all ± 200.

A. Electrical and thermal resistivities

The transverse electrical resistivity ρ_{xx} does not significantly affect the following analysis or conclusions, but it is useful to present the data for the sake of completeness. Measurements on samples 2 and 3 showed ρ_{xx} to be linear in magnetic field (the usual observation) and the dependence can be characterized by Kohler slopes[25] of $S = (0.94 \pm 0.07) \times 10^{-2}$ (sample 2) and $(1.15 \pm 0.06) \times 10^{-2}$ (sample 3). We have only one value of $\rho_{xx}(B, T)$ for sample 1 (taken at 3.25 T and 4.2 K) other than $\rho_{xx}(0, 4.2\ \mathrm{K})$, and on the assumption that $\rho_{xx}(B)$ is again linear we find $S = (2.5 \pm 0.5) \times 10^{-3}$ for this sample.

Figures 2 and 3 give a representative set of our data on the transverse thermal magnetoresistivity γ_{xx}, and the Righi-Leduc resistivity γ_{yx} (presented in the form $\gamma_{yx} L_0 T/B$). The data are very similar for all three samples. We see that γ_{xx} has the same general features as observed in previous work,[1,5-7] and can be accurately represented ($\sim 0.2\%$) by expressions of the form

$$\gamma_{xx} = a_0 + a_1 B + a_2 B^2 . \tag{5}$$

However, we have not made use of this equation in the analysis and we shall not reproduce the coefficients here.

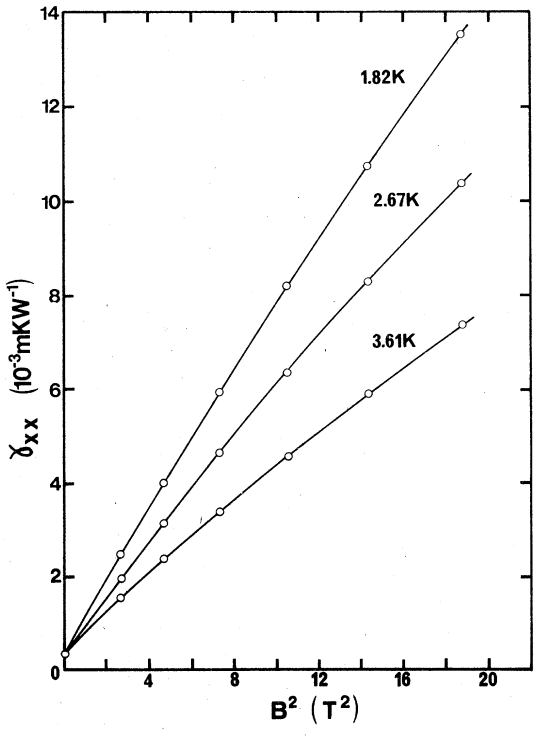

FIG. 2. Thermal magnetoresistivity γ_{xx} of sample 1, shown as a function of B^2, for three different temperatures. Samples 2 and 3 give very similar results. Notice that the lines through the data are not straight.

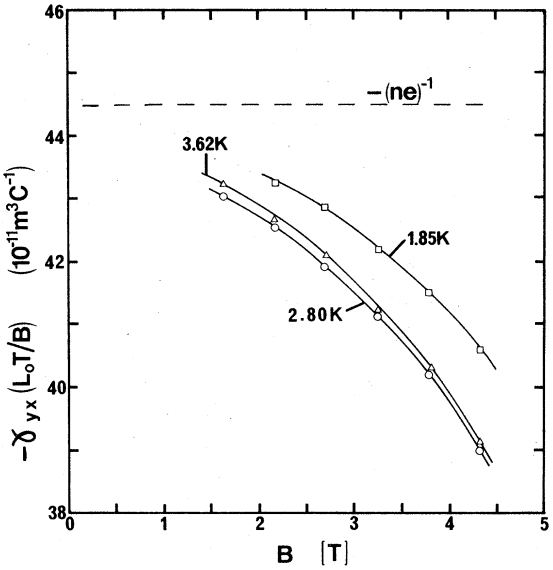

FIG. 3. Righi-Leduc resistivity γ_{yx} of sample 2 (multiplied by $L_0 T/B$) as a function of B at three different temperatures. Samples 1 and 3 give similar results. Dashed line labeled $-(ne)^{-1}$ is the theoretical value of $-\gamma_{yx}(L_0 T/B)$ if the lattice conductivity is zero.

It will be noted from Fig. 3 that $|\gamma_{yx}| L_0 T/B$ drops rather rapidly as B is increased, contrary to previous results.[7] In the absence of any lattice thermal conductivity, theory predicts[4] that in the high-field limit $\gamma_{yx} L_0 T/B$ will have the simple value $(ne)^{-1}$, i.e., the horizontal dashed line in Fig. 3. If λ^g is included, the theory then predicts[2] a steady decrease of $|\gamma_{yx}| L_0 T/B$ away from $(n|e|)^{-1}$, and at the same time produces an increase in γ_{xx} which to first order is $\sim B^2$ (Sec. I); qualitatively our results show exactly these features, but it remains to be seen whether a quantitative fit can be made.

The simplest and most convincing way to check if λ^g is indeed responsible for all the effects is to use the measured components of $\vec{\gamma}$ to obtain those of $\vec{\lambda}$. It is important to notice that *although the behavior of both γ_{xx} and γ_{yx} are modified by λ^g, the predicted value of λ_{xy} is completely unaffected and is simply given by $\lambda^e_{xy} = L_0 Tne/B$.* Figure 4 presents our results on $\lambda_{xy} = \gamma_{yx}/(\gamma_{yx}^2 + \gamma_{xx}^2)$ plotted in the form of $L_0 T/\lambda_{xy} B$ for comparison with $(ne)^{-1}$. The systematic errors (mainly from thickness determinations) associated with $L_0 T/\lambda_{xy} B$ could be as high as 3%, but the internal consistency should be much better at perhaps ± 1% (arising mainly from thermometer calculations; however, about 0.4% is due to dimensional errors that become a function of B owing to γ_{xx}^2 and γ_{yx}^2 having different weighting at different fields).

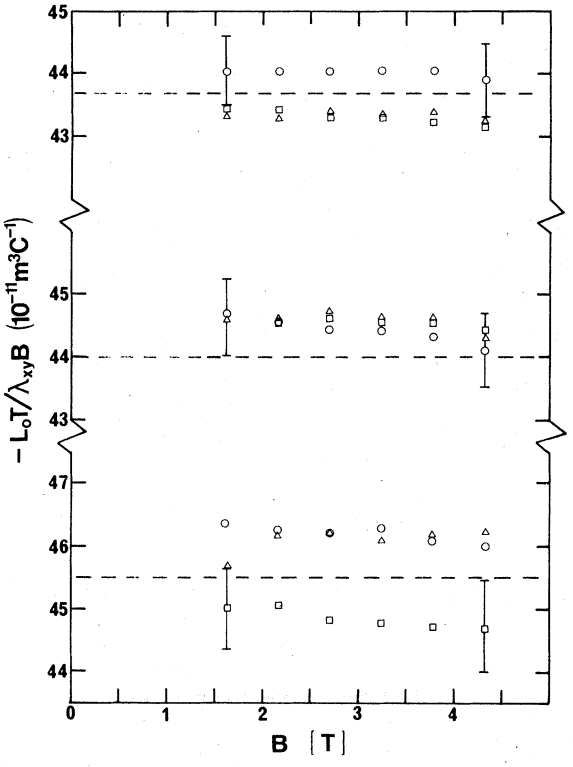

FIG. 4. Inverse of the Righi-Leduc conductivity λ_{xy} of all three samples (derived from data the same or similar to those of Figs. 2 and 3) multiplied by L_0T/B and presented as a function of B. From top to bottom the results are for samples 1, 2, and 3, respectively. The symbols represent: for sample 1, ○ 3.60 K, △ 2.67 K, □ 1.82 K; for sample 2, ○ 3.60 K, △ 2.80 K, □ 1.85 K; for sample 3, ○ 3.74 K, △ 2.89 K, □ 1.94 K. Dashed lines give the values of the Hall conductivities measured on the same samples. Expected high-field value of both $(\sigma_{xy}B)^{-1}$ and $L_0T/\lambda_{xy}B$ is $(ne)^{-1} = -44.5\times10^{-11}$ m^{3}C^{-1}.

Most of the experimental data lie within 2% of the expected value $(ne)^{-1}$. Furthermore, because the relative accuracy of the data is better than the absolute accuracy, we are able to verify that $\lambda_{xy} \propto T$ within 1% and $\lambda_{xy} \propto B^{-1}$ to 0.5%.

Sample 3 shows some variations from run to run which are not completely understood. There appear to be changes in the absolute magnitude $L_0T/\lambda_{xy}B$ of about 2% between the various sets of data, which is on the limit of experimental error. These discrepancies occurred after the sample had been warmed to room temperature to repair a vacuum seal. (This was not necessary for samples 1 and 2.) At such times we usually squeeze down the clamps to maintain good electrical and thermal contact—and it is possible that the sample may be slightly stretched during this process. Since all thickness measurements are made after sample demounting, it may be that the thickness used in reducing the earlier data is in fact incorrect (the sample being slightly thicker at that time). In any event, the variations are not so large as to be a serious cause for concern.

The experimental data tend to be vertically displaced from $(ne)^{-1}$, and we presume that such trends are at least partly due to unavoidable errors incurred in measuring the sample thicknesses. To check this, we have determined the Hall resistivities ρ_{yx} of our samples and we have used them to calculate the Hall conductivities σ_{xy}. In practice $\rho_{xx}^2 \ll \rho_{yx}^2$ and with negligible error we have $\sigma_{xy} = \rho_{yx}^{-1}$. The predicted[26] value of σ_{xy} is ne/B, independent of T, and we have plotted $1/\sigma_{xy}B$ in Fig. 4 for comparison with $L_0T/\lambda_{xy}B$. Errors in sample thickness will have the same effect on the two quantities (but we should recall that, contrary to the case of σ_{xy}, it is *not* true to assume $\gamma_{yx}^2 \gg \gamma_{xx}^2$ and dimensional uncertainties in γ_{xx} will reveal themselves as systematic changes in λ_{xy}, ~ 0.4% typically, as a function of B). Nevertheless, the agreement between the galvano- and thermomagnetic data is generally excellent with differences of usually ≤ 1%. We believe that these residual discrepancies simply reflect the accuracy of the calibrations of the carbon thermometers; it would be difficult to reduce their magnitude by a significant factor.

The previous results of Tausch and Newrock[7] exhibited a 15–20% drop in $\lambda_{xy}B/L_0T$ by 4.5 T. As we have noted, we find $\lambda_{xy}B$ to be constant to about 0.5% up to 4.5 T. Clearly the two sets of data are contradictory.

There are two immediate conclusions that may be drawn from this analysis:

(i) The results show that $\sigma_{xy} = \lambda_{xy}/L_0T$ to an accuracy of about 1%. Speculation[7] that $\gamma_{yx}^e L_0T \neq \rho_{yx}$ in the high-field limit is unfounded (γ_{yx}^e is the value that γ_{yx} would have if $\lambda^g = 0$ and is just λ_{xy}^{-1} to high accuracy). The results further show that both $1/\sigma_{xy}B$ and $L_0T/\lambda_{xy}B$ have the predicted values of $(ne)^{-1}$ to within the experimental accuracies of about 2% and 3% respectively.

(ii) That such an unusual behavior of γ_{yx} and γ_{xx} proves to yield such remarkably well-behaved λ_{xy} gives us confidence in our experimental techniques and error limits.

We now turn our attention to the diagonal component λ_{xx}. *Notice that exactly the same data that were used to evaluate* λ_{xy} *are also used to obtain* $\lambda_{xx} = \gamma_{xx}/(\gamma_{xx}^2 + \gamma_{yx}^2)$. When λ^g is added to λ_{xx}^e [Eq. 2(a)], then λ_{xx} should have the form

$$\lambda_{xx} = \alpha(T)/B^2 + \lambda^g \ . \tag{6}$$

Figure 5 shows some of our data on λ_{xx} as a function of B^{-2}; the graphs produce good straight lines from which $\alpha(T)$ and λ^g can be immediately obtain-

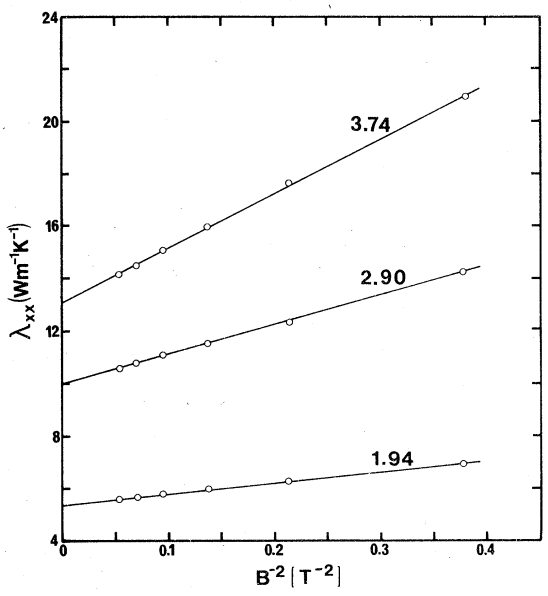

FIG. 5. Thermal conductivity λ_{xx} (evaluated from data similar to those of Figs. 2 and 3) of sample 3 plotted as a function of B^{-2} for three different temperatures. Results on samples 1 and 2 are very similar.

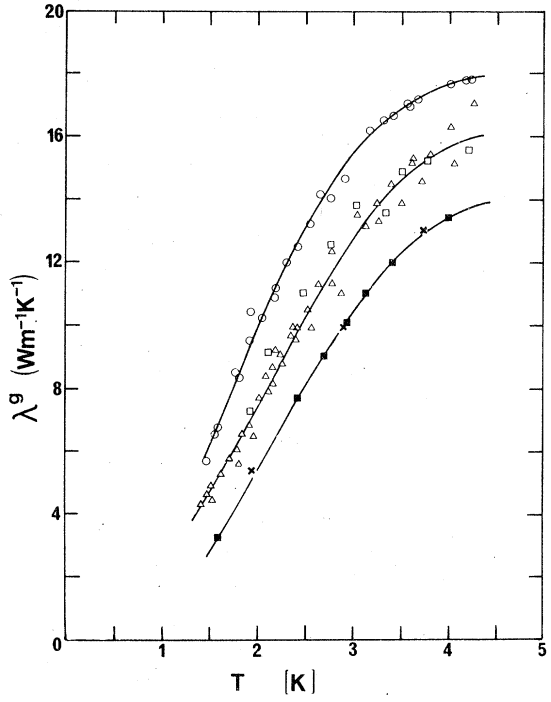

FIG. 6. Temperature dependence of the lattice thermal conductivity λ^g of each sample. The symbols represent: ○ sample 1; △ sample 2; □ sample 3 initial data; ■ sample 3 during second series of experiments (after having been warmed to room temperature); × sample 3 during the third series of experiments, having been warmed to room temperature twice.

ed. Figure 6 gives all our data on λ^g. However, only a fraction of these data was actually obtained in exactly the above manner. In practice it is very time consuming to take all the data necessary to perform the inversions of $\vec{\vec{\gamma}}$ as a function of B and T. Thus for each sample we take complete "master" sets from about 1.5 to 4.5 T for three different temperatures between 1.5 and 4.5 K. A great quantity of data is then taken at finely spaced temperatures (but only for one high-field value, typically 3.25 T), where λ_{xx} is not much larger than λ^g. Using the master sets we produce an interpolation graph for $\alpha(T)$ and are thus able to correct all the data for the relatively small effects of λ^e_{xx} and obtain λ^g. Figure 7 gives $\alpha(T)$ in the form of $\alpha(T)/T$ against T^3 for our samples.

Before discussing λ^g and $\alpha(T)$, it is prudent to examine other possible terms which might contribute to Eq. (6) and the possible errors in the derived quantities. The inversions tend to compound small errors and we expect λ_{xx} to be absolutely accurate only to about 5%. However for a single sample at constant T the relative errors as a function of B should be only 0.5% with random errors ~ 0.5%, and at constant B the relative errors as a function of T should be ~1.5%. Unfortunately, there are more subtle sources of error. Thus we were somewhat surprised that the data

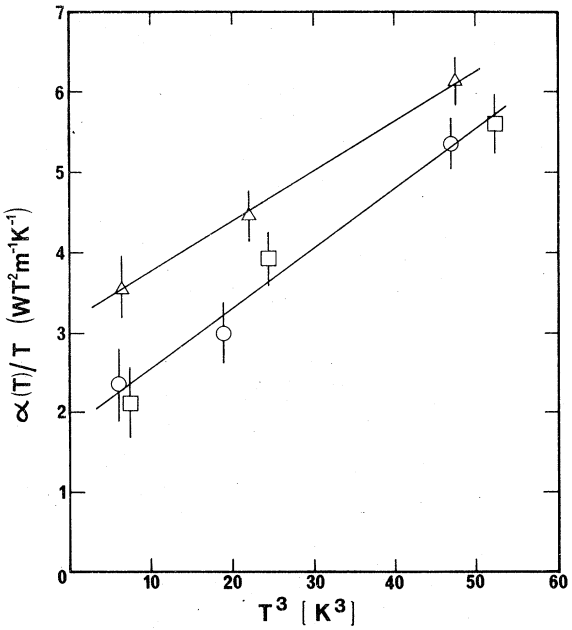

FIG. 7. Slopes $\alpha(T)$ of the lines of Fig. 5 (and other similar results), divided by T, and plotted as a function of T^3 for the three samples. The symbols represent ○ sample 1; △ sample 2; □ sample 3 (on third cooldown). Errors do not take into account the possible presence of a term $\beta(T)/B$ in λ_{xx} (see text).

on λ_{xx} could be so accurately fitted to Eq. (6), the fits usually being accurate to < 1%. Previous work[27] on Pb had led us to expect the possible presence of a term in B^{-4}, and other work[28] on the uncompensated metals Al and In had demonstrated the necessity of a term in B^{-1}. It is straightforward to show that the B^{-4} term should be very small. If we ignore scattering anisotropy we can approximate

$$\lambda_{xx}^{e} \sim \lambda_0^e/(1+\omega^2\tau_{\rm th}^2) \ , \tag{7}$$

where λ_0^e is the zero-field electronic thermal conductivity, ω the cyclotron frequency and $\tau_{\rm th}$ the thermal relaxation time ($\omega\tau_{\rm th} \sim \lambda_0^e B/L_0 Tn|e|$). Expanding Eq. (7) enables us to estimate the ratio of the coefficients of the B^{-2} and B^{-4} terms and we find that the B^{-4} term should be completely negligible for all our samples in the field and temperature range that we have considered.

The term[28] in B^{-1}, say $\beta(T)/B$, originates from a term linear in B in γ_{xx}^e (again this is γ_{xx} if $\lambda^g = 0$), which will presumably be present by analogy with the electrical magnetoresistance.[1,5,28] If the linear term is assumed to arise from the presence of inhomogeneities, voids, etc., as seems likely, then it has been shown within the approximations of a particular model,[29] that although γ_{xx}^e would exhibit such a linear term, the presence of λ^g modifies this dramatically. In particular the "linear term" that would be observed in γ_{xx} is no longer linear in B but tends to saturate.

We have attempted to fit our data with an equation of the form

$$\lambda_{xx} = \lambda^g + \beta(T)/B + \alpha(T)/B^2 \ . \tag{8}$$

With an extra free parameter $\beta(T)$, the data fits can always be improved but the improvement is in fact marginal in all cases. The coefficient $\beta(T)$ usually lies between $\pm$ 5 W T m^{-1} K^{-1}, but the fact that it is observed to randomly take either sign is clearly inconsistent with the assumed origin. The most likely explanation is that the magnitude of $\beta(T)$ reflects mainly the random and systematic errors in λ_{xx}. We must conclude that if $\beta(T)/B$ is present, then $|\beta(T)| \leq 5$ W T m^{-1} K^{-1}.

Newrock and Maxfield[6] fitted their data on γ_{xx} to an expression equivalent to Eq. (5) and found $a_1 \sim 10^{-4}$ mK W^{-1} T^{-1} at 2 K increasing to about 3 $\times 10^{-4}$ mK W^{-1} T^{-1} at 4.2 K. Thus at 4 K we expect $\beta(T) \sim a_1(L_0 neT)^2 \sim 15$ W T m^{-1} K^{-1}. A term of this magnitude is definitely not present in our data and may be taken as an indication that the linear term does disappear with increasing B for finite λ^g in agreement with theory.[29] However, we believe that such a conclusion should be more thoroughly tested by measuring the linear terms on the *same* samples at high and low fields.

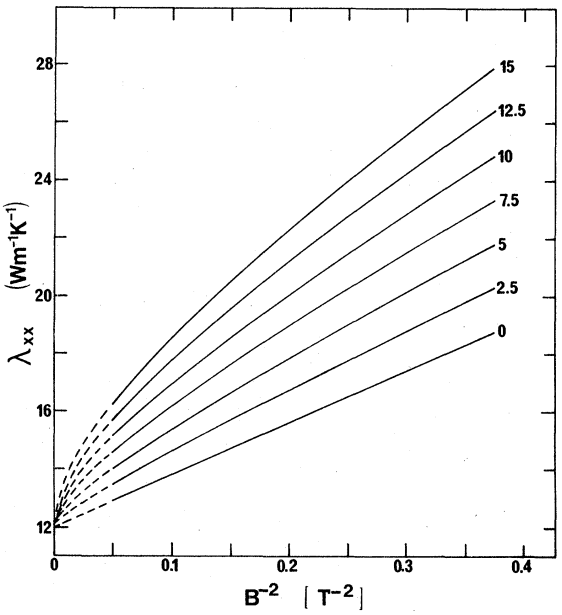

FIG. 8. Calculated curves of λ_{xx} assuming it to be of the form $\lambda_{xx} = \lambda^g + \beta(T)/B + \alpha(T)/B^2$. We have used the data on λ^g and $\alpha(T)$ appropriate to one of the samples at about 3 K [$\lambda^g = 12$ W m^{-1} K^{-1}, $\alpha(T) = 18$ W T^2 m^{-1} K^{-1}]. Values of $\beta(T)$ are given on the curves in units of W T m^{-1}. For $\beta(T) \gtrsim 5$ W T m^{-1}, the lines become so curved over the experimental field range (shown as solid lines) as to be easily noticeable on the data. By comparing with the actual data (e.g., Fig. 5) we conclude $\beta(T) \leq 5$ W T m^{-1} for all our samples at all temperatures.

Nevertheless the possible presence of a linear term can introduce errors into $\alpha(T)$ and λ^g. To illustrate this, we have plotted in Fig. 8 λ_{xx} according to Eq. (8) with $\lambda^g = 12$ W m^{-1} K^{-1}, $\alpha(T) = 18$ W T^2 m^{-1} K^{-1}, and various values of $\beta(T)$ from 0 to 15 W T m^{-1} K^{-1}. For $\beta(T) \lesssim 5$ W T m^{-1} K^{-1} and for our range of B, the curves can be accurately approximated by ignoring the B^{-1} term and retaining only $\lambda^g + \alpha(T)/B^2$ but the values of λ^g and $\alpha(T)$ so obtained will be too high. In fact λ^g increases by about ~1W m^{-1}K^{-1} and $\alpha(T)$ by ~5.5 WT^2 m^{-1}K^{-1} for the upper limit on $\beta(T)$ of 5 W T m^{-1}K^{-1}, though the straight-line fit would never depart by more than 0.5% from the true curve.

We conclude from this that the possible presence of a term $\beta(T)/B$ with $\beta(T) \lesssim 5$ W T m^{-1}K^{-1} cannot be discounted, and this implies that the λ^g in Fig. 6 might be systematically too high by $\lesssim 1$ W m^{-1}K^{-1} and $\alpha(T)$ in Fig. 7 might be too high by $\lesssim 5$ W T^2 m^{-1}K^{-1}. With this in mind, we return to the discussion of $\alpha(T)$ and λ^g.

In view of the free-electron-like character of potassium it seems reasonable to estimate $\alpha(T)$ within the approximations of the free-electron

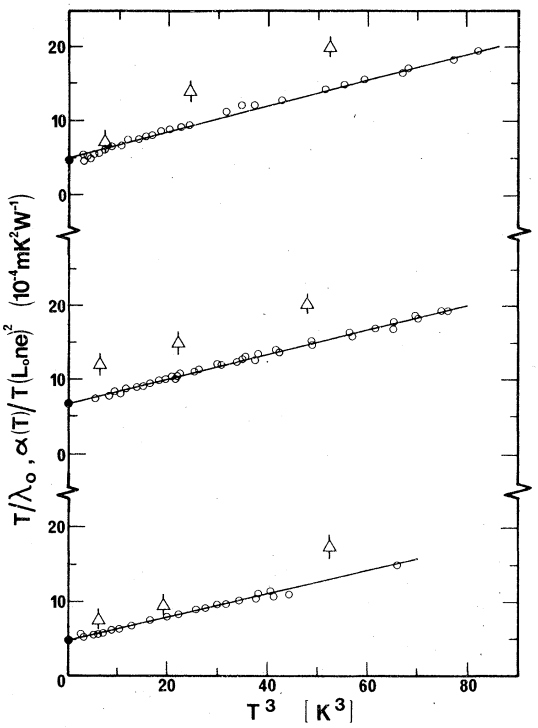

FIG. 9. Zero-field thermal conductivity λ_0 shown in the form of T/λ_0 vs T^3 for the three samples (open circles and lines). From bottom to top the results are for samples 1, 2, and 3, respectively. The solid circles on the ordinate axis give ρ_0/L_0, where ρ_0 is the measured residual resistivity in zero field. Triangles give the data on $\alpha(T)/(L_0 Tne)^2$ and are the same data as appear in Fig. 7 (after multiplying by $(L_0 Tne)^{-2}$.

model. In the high-field limit, Eq. (7) (which we recall ignores the anisotropy of the electronic scattering) reduces to $\lambda_{xx}^e = \lambda_0^e/(\omega\tau_{th})^2$. The same model gives

$$\lambda_{xy} = \lambda_0^e/\omega\tau_{th} = L_0 Tn|e|/B ,$$

from which we immediately find

$$\lambda_0^e \alpha(T) = (L_0 Tne)^2 . \tag{9}$$

To enable a check to be made on the validity of Eq. (9), we have measured[30] the zero-field thermal conductivity λ_0, which is equal to λ_0^e to within 0.5% for our samples, and in Fig. 9 we have plotted both $\alpha(T)/T(L_0 ne)^2$ and T/λ_0 as a function of T^3. The graphs are plotted in this form because we expect that within the Matthiessen's rule approximation $(\lambda_0^e)^{-1} = a/T + bT^2$, where the term a/T results from impurity scattering (and should be equal to $\rho_0/L_0 T$, where ρ_0 is the residual resistivity) and the term bT^2 arises from phonon scattering; thus $T/\lambda_0^e = a + bT^3$. We notice in passing that the intercepts of T/λ_0 in Fig. 9 are indeed equal to ρ_0/L_0 to within the experimental accuracies. Equation (9) shows $\alpha(T)/T$ should have the same form as T/λ_0^e; more general arguments[31] also indicate that $\alpha(T)/T$ will be the sum of a constant plus a term in T^3, though in general the ratio of the coefficients is not necessarily the same as those describing T/λ_0^e.

From Fig. 9 it is seen that both T/λ_0 and $\alpha(T)/T$ do show the expected temperature dependences, within experimental error, but it is clear that Eq. (9) can be regarded only as a first approximation. It is possible that some of the discrepancy is simply due to the effects of a residual $\beta(T)/B$ term as we have discussed earlier but at the higher temperatures such effects should be small. We have no explanation of any remaining differences.

A few comments about λ^g are in order, though we shall reserve most of our discussion for Secs. IV and V. The absolute accuracy of the λ^g data is about 7% (ignoring the possible effects of a B^{-1} term), but a single sample will be internally consistent to about 4% over the whole temperature range. Below about 3 K, the present results on λ^g are in good agreement with those deduced from the earlier low-field data[1] on γ_{xx} (using the method discussed in Sec. I). In retrospect we realize that some of the approximations which were made in the early analysis were not always sufficiently good. In particular we believe that the falloff of λ^g that those results showed above 3 K is not real but originates from the approximation that $\gamma_{yx} = B/L_0 Tne$. This approximation can be rather poor for $B < 1$ T at these higher temperatures but improves dramatically at the lower temperatures.[17,32] The present results do not rely on these approximations, though as a matter of fact they are accurate for the field range we have used here.

Using only the free-electron model and our derived values of λ^g, we can reproduce the experimental curves on γ_{xx} and γ_{yx} with good accuracy. Thus with $\lambda_{xx}^e = \lambda_0^e/(1+\omega^2\tau_{th}^2)$, $\lambda_{xy}^e = \lambda_0^e\omega\tau_{th}/(1+\omega^2\tau_{th}^2)$, and $\omega\tau_{th} = \lambda_0^e B/L_0 Tn|e|$, then one can show that

$$\gamma_{xx} = \frac{\lambda_0^{-1} + \lambda^g(\lambda_0^e/\lambda_0)^2(B/L_0 Tne)^2}{1 + (\lambda_0^e/\lambda_0)^2(\lambda^g B/L_0 Tne)^2} , \tag{10a}$$

$$\gamma_{yx} = \frac{(\lambda_0^e/\lambda_0)^2 B/L_0 Tne}{1 + (\lambda_0^e/\lambda_0)^2(\lambda^g B/L_0 Tne)^2} . \tag{10b}$$

These are just special cases of more general equations.[2] Taking the values of λ^g from the intercepts of Fig. 5, we have evaluated Eqs. (10a) and (10b) and Figs. 10(a) and 10(b) show the calculated and experimental data for sample 2. The equations reproduce the data surprisingly accurately and, in particular, we see that the slight deviations from a perfect B^2 dependence of γ_{xx} are both predicted and measured.

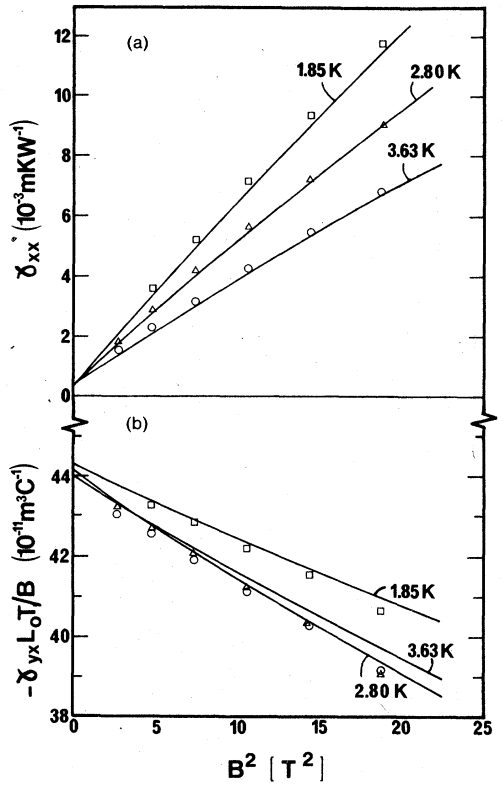

FIG. 10. Fits to γ_{xx} (a) and γ_{yx} (b) of sample 2 using Eqs. (10a) and (10b). The only free parameter is λ^e, which is taken from Fig. 5. The quality of the fits on samples 1 and 3 is similar.

However, we should not read too closely into the accuracy of the fit in an effort to prove that K is accurately free electronlike. Thus at fields above ~1T, Eq. (10a) is dominated by the term in the numerator $\lambda^e(B/L_0Tne)^2$ (recalling that $\lambda_0^e/\lambda_0 \sim 0.99$) and the correction terms in both denominators have a similar form, i.e., $(\lambda^e B/L_0Tne)^2$. The important point is that these major terms *do not depend on* τ_{th} [and hence on $\alpha(T)$] and derive essentially from the accuracy with which $\lambda_{xy} = L_0Tne/B$. Since we know that this relation is obeyed extremely well, and since we obtain λ^e from the same data that we are fitting, it is not surprising that the equations reproduce the data so well. In fact the way we chose λ^e forces the curves of Figs. 10(a) and 10(b) to fit the data almost perfectly at the highest field; at the same time, the curves must fit the zero-field value of γ_{xx} since the leading term of Eq. (10a), i.e., λ_0^{-1}, is an experimental measurement. Nevertheless, the accuracy of the fits remains impressive when we bear in mind that it uses only two parameters, λ_0 and λ^e, and the former is a fixed quantity taken directly from experiment.

To briefly summarize this section, we believe that we have proved beyond any reasonable doubt that the observed field variations in γ_{xx} and γ_{yx} are *completely* accounted for by the presence of a constant term in the diagonal components of $\vec{\lambda}$. The simplest reasonable identification of this term is that it represents the lattice thermal conductivity λ^e. This conclusion is just the opposite to that drawn by Tausch and Newrock[7]. Although their data are superficially similar to ours, we agree with them that they cannot be consistently analyzed in the manner that we have presented. However in view of the very large discrepancy between their values of λ_{xy} and the predicted value of L_0Tne/B, one must have serious doubts that their data represent the actual behavior of potassium.

B. Thermoelectric properties

In this section we first present our data on ϵ_{yx}''; this will be followed by those on the zero-field thermopower S, and finally we show some data on the field variation of the thermopower.

We obtain ϵ_{yx}'' by studying the Nernst-Ettingshausen coefficient $P^a = E_y/U_x$. It is readily shown that with the conditions $U_y = 0 = U_z$ and $\vec{J} = 0$,

$$P^a = \epsilon_{yx}''(\rho_{xx}\gamma_{xx} - \gamma_{yx}\rho_{yx}) + \epsilon_{xx}''(\rho_{yx}\gamma_{xx} + \gamma_{yx}\rho_{xx}) . \quad (11)$$

In the high-field limit, the term $-\epsilon_{yx}''\rho_{yx}\gamma_{yx}$ dominates the others and we can show from our data that all the remaining terms contribute less than 1% for the range of field and temperature in which we are working. As with the Hall and Righi-Leduc resistivities, an accurate measure of the sample thickness is needed in order to determine P^a. However, if we are willing to assume that ρ_{yx} has a known value (in our case we take this to be B/ne), and if we measure P^a and γ_{yx} on the same sample, then it is readily shown that the value of ϵ_{yx}'' we deduce from $\epsilon_{yx}'' = P^a ne/\gamma_{yx}B$ is independent of the sample thickness. Figure 11 gives some of our data on $\epsilon_{yx}''B/T$ as a function of B and verifies, within experimental error, the expected relationship $\epsilon_{yx}'' \propto B^{-1}$. Figure 12 presents our results on $\epsilon_{yx}''B/T$ as a function of T for the three samples. There should not be any appreciable systematic errors in these data (say < 1%) since we already know that γ_{yx} produces accurate values of λ_{xy}, and the only other sources of uncertainty are the gain of the superconducting chopper amplifier and the heater powers, both of which are known to about 0.1%.

We shall postpone our detailed discussion of the results until Secs. IV and V, but a few general comments are in order at this point. As we mentioned in the Introduction, the high-field limiting result[12] for the diffusion part ϵ_{yx}^d is $\gamma T/B$ and we can accurately predict its value from available

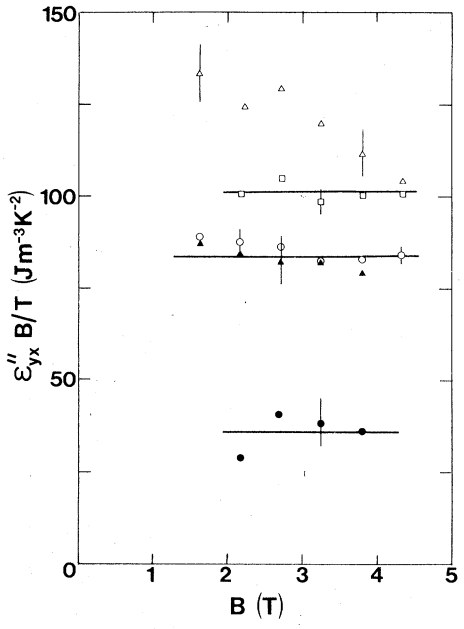

FIG. 11. Data on the field dependence of ϵ''_{yx} for samples 1 and 2 plotted in the form $\epsilon''_{yx}B/T$ vs B. The symbols represent: sample 1, ○ 3.63 K; △ 2.80 K; □ 1.85 K; sample 2, ● 4.3 K, ▲ 3.8 K. Nonconstancy of the 2.80 K data was probably due to temperature variations during the experiments.

specific-heat results. The horizontal line of Fig. 12 is just the experimental value[33] of γ. The crucial point is that any deviations of $\epsilon''_{yx}B/T$ from γ can be attributed only to phonon drag, i.e., $\epsilon^{g}_{yx}B/T$. There are no doubts in this identification, as for instance often occur in the analysis of the zero-field thermopower. We believe that this is the most direct and unambiguous demonstration of the presence of phonon drag in any transport property of potassium.

We can go further. Opsal's theoretical results[34] on ϵ^{g}_{yx} take a particularly simple form for the case of a simple Fermi surface, such as that of potassium. It is found that normal electron-phonon scattering always gives rise to a positive contribution to ϵ^{g}_{yx}, while umklapp electron-phonon scattering produces a negative contribution. (Such a simple classification cannot be made for all the other metals so far studied; See Ref. 12 for some of these metals.) Thus we are able to identify the initial rise in $\epsilon^{g}_{yx}B/T$ in Fig. 12 as being due to the normal processes, and the rapid turnover beginning near 2 K as reflecting the onset of umklapp processes. This identification is also unambiguous and shows quite clearly the temperature at which umklapp processes first become significant for K.

Figure 13 presents our data on the zero-field thermopower of samples 2 and 3; we were unable to obtain any results for sample 1. We show later (Sec. IV and V) that the negative peak has exact-

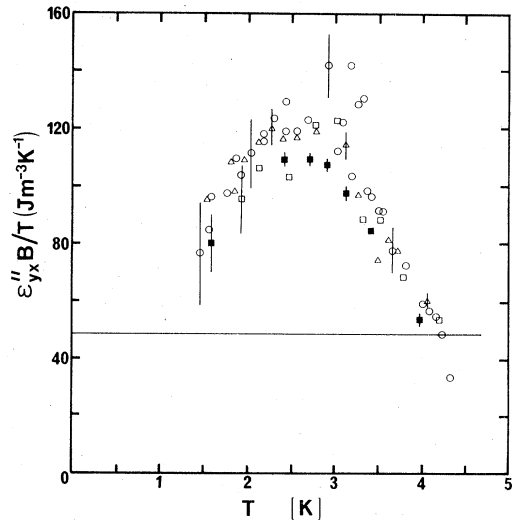

FIG. 12. All the data on $\epsilon''_{yx}B/T$ for the three samples as a function of T. The symbols represent: ○ sample 1; △ sample 2; □ sample 3 (first series); ■ sample 3 (third series) after warming to room termperature twice. The horizontal line shows the coefficient of the electronic specific heat γ; $\epsilon''_{yx}B/T$ would have the constant value γ if phonon drag were absent.

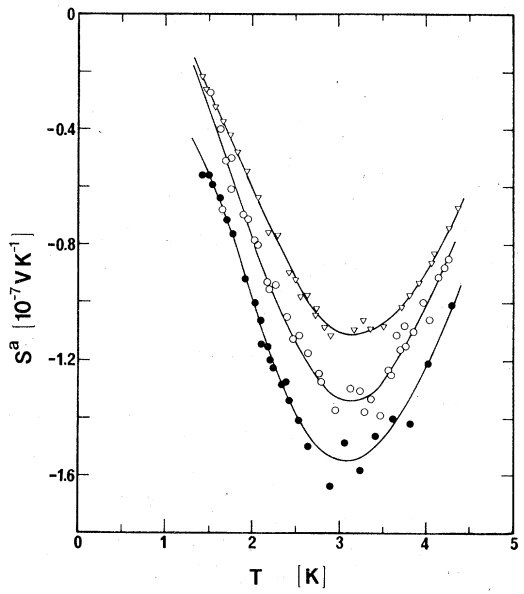

FIG. 13. Thermopowers of samples 2 and 3. The symbols represent: ○ sample 2 at $B=0$; ● sample 2 at $B=3.25$ T; ▽ sample 3 at $B=0$. Data on sample 3 were taken during the third series of experiments after warming the sample twice to room temperature.

ly the same origin as the positive peak in ϵ''_{yx}. The initial (negative) rise of S is due to the electron-phonon normal processes contributing to S^g, together with a diffusion term nearly linear in T, and the rapid turnover again reflects the onset of the electron-phonon umklapp-scattering contribution to S^g.

The features displayed by our data on S are in good qualitative agreement with the earlier results of MacDonald *et al.*[35] Both sets of results exhibit negative peaks at about the same temperature ~ 3 K, but the earlier data have a peak of smaller magnitude. We believe that the discrepancies are not due to experimental error, but arise from the fact that the early data were taken on samples constrained in tubes; as the samples cooled, the differential contraction between the sample and tube would severly strain the sample and lead to large dislocation densities. Phonon-dislocation scattering then reduces the size of the negative peak.

The adiabatic thermopower $S^a[=E_x/(\partial T/\partial x)$ with $\vec{J}=0$ and $U_y=0=U_z]$ is the quantity actually measured as a function of field. Figures 13 and 14 show our results on S^a for sample 2. Because, as we shall show, S^a is not a particularly useful quantity for K, we did not attempt to take data on sample 3. Other metals have generally shown[36] strong variations of S^a with B, and, in contrast, the present data are remarkable for the lack of any pronounced variation.

Equations (1a) and (1b) immediately yield

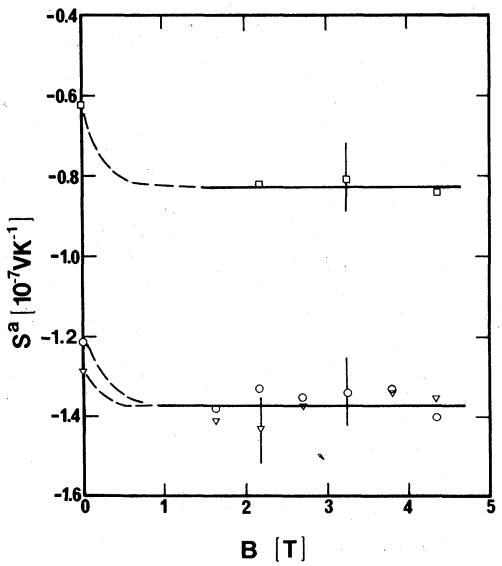

FIG. 14. Thermopower of sample 2 as a function of B. The symbols represent: ○ 3.63 K, ▽ 2.84 K, □ 1.84 K. Dashed lines to the points at $B=0$ are tentative interpolations to indicate the trend of the data.

$$S^a=-\epsilon''_{xx}(\rho_{xx}-\gamma_{yx}\rho_{yx}/\gamma_{xx})+\epsilon''_{yx}(\rho_{yx}+\gamma_{yx}\rho_{xx}/\gamma_{xx})\,. \quad (12)$$

As $B\to 0$, $S^a\to S=-\epsilon''_{xx}\rho_{xx}$. If λ^g were small, it would not have been possible to determine which, if any, of the last three terms would be most important at high fields since they would all tend to constants ($-\rho_{xx}\epsilon''_{xx}$ can be safely dismissed as this term would be $\sim B^{-2}$, or perhaps between B^{-1} and B^{-2} if ρ_{xx} exhibits a linear magnetoresistance term). However, as we have seen, the presence of a finite λ^g will always result in a term in γ_{xx} of the order B^2. In potassium we have shown that λ^g is anomalously large and its presence modifies γ_{xx} enormously so that the B^2 term is very large and dominates the behavior of γ_{xx}. Thus the terms $\gamma_{yx}\rho_{yx}\epsilon''_{xx}/\gamma_{xx}$ and $\gamma_{yx}\rho_{xx}\epsilon''_{yx}/\gamma_{xx}$ rapidly decrease, leaving only $\rho_{yx}\epsilon''_{yx}$.

We can be more quantitative. Having taken extensive data on P^a, S^a, ρ_{xx}, ρ_{yx}, γ_{xx}, and γ_{yx} for sample 2, it is a simple matter to solve Eqs. (11) and (12) to determine the relative weighting of the various terms. This procedure yields the interesting result that the terms $\epsilon''_{xx}\rho_{yx}(\gamma_{yx}/\gamma_{xx})$ and $\epsilon''_{yx}\rho_{xx}$ $(\gamma_{yx}/\gamma_{xx})$ have very nearly the same magnitude but are of opposite sign for the range of temperatures and fields that we have investigated. By 3.25 T, the field at which the data of Fig. 13 were taken, these terms each comprise about 10% of the total but their sum is $\leq 2\%$. This near cancellation is not coincidental and originates in the free-electron-like character of potassium. If one examines the free-electron expressions[37] for $\epsilon''_{xx}\rho_{yx}$ and $\epsilon''_{yx}\rho_{xx}$, including full phonon drag from normal electron-phonon scattering, one finds that in the high-field limit they should be equal and opposite provided we can ignore the presence of the contribution involving the energy derivatives of the relaxation time $\partial\tau/\partial\mu$ in the diffusion part of ϵ''_{xx}.

The end result of this is that S^a is practically equal to $\epsilon''_{yx}\rho_{yx}$ at high fields, to an accuracy of $\leq 2\%$. Thus S^a does not give us much new information. However, the experimental correlation between the zero-field thermopower $S=(\epsilon''_{xx}\rho_{xx})_{B=0}$ and the high-field thermopower $S^a\approx(\epsilon''_{yx}\rho_{yx})_{B\to\infty}$ is forcefully brought to our attention. The reason for the similarity is not difficult to find and is very revealing. It is readily shown that $(\epsilon''_{xx}\rho_{xx})_{B=0}$ and $(\epsilon''_{yx}\rho_{yx})_{B\to\infty}$ would be identical for the free-electron model,[37] including full phonon drag due to normal electron-phonon scattering, except for the term involving $\partial\tau/\partial\mu$ in $(\epsilon''_{xx})_{B=0}$. We are led to suggest that this energy derivative does not play a major role in S.

IV. THEORY

In this section we briefly outline the derivation of the expression used to calculate the low-tem-

perature phonon conductivity of potassium. We also discuss the derivation of the very different expression used by Ekin[10] in his calculation.

To calculate the zero-field thermal conductivity of a cubic metal we first determine the electron and phonon distribution functions, f and n respectively, in the presence of a uniform temperature gradient in a high-symmetry direction, say $\vec{\nabla}T = \nabla T\hat{x}$. In the usual way,[38] we write

$$f_{\vec{k}} \equiv f^0_{\vec{k}} - \Phi_{\vec{k}} \frac{\partial f^0_{\vec{k}}}{\partial \epsilon_{\vec{k}}} \tag{13}$$

and

$$n_{\vec{q}j} \equiv n^0_{\vec{q}j} - \Psi_{\vec{q}j} \frac{\partial n^0_{\vec{q}j}}{\partial \hbar\omega_{\vec{q}j}} . \tag{14}$$

Here $\epsilon_{\vec{k}}$ is the energy (measured relative to the chemical potential) of the electron with wavevector $\vec{k}$; $\omega_{\vec{q}j}$ is the frequency of the phonon with wavevector $\vec{q}$ and polarization index j. $f^0_{\vec{k}}$ and $n^0_{\vec{q}j}$ are the Fermi and Bose distribution functions respectively. The steady-state phonon Boltzmann equation[38,39] is

$$\left(\frac{\nabla T}{T}\right)\hbar\omega_{\vec{q}j} n^0_{\vec{q}j}(1+n^0_{\vec{q}j}) u_{\vec{q}jx} + \sum_{\vec{k},\vec{k}'} (\Phi_{\vec{k}} - \Phi_{\vec{k}'} + \Psi_{\vec{q}j}) P^{p-e}_{\vec{k},\vec{q}j;\vec{k}'} + \Psi_{\vec{q}j} n^0_{\vec{q}j}(1+n^0_{\vec{q}j}) \sum_{r\neq e} (\tau^{p-r}_{\vec{q}j})^{-1} = 0. \tag{15}$$

$\vec{u}_{\vec{q}j} \equiv \partial\omega_{\vec{q}j}/\partial\vec{q}$ is the phonon group velocity. In the term describing the effect of phonon-electron $(p-e)$ scattering, the transition rate for the process $\vec{k} + \vec{q}j \to \vec{k}'$ is given by[38]

$$P^{p-e}_{\vec{k},\vec{q}j;\vec{k}'} = \frac{2\pi}{\hbar} \sum_i |g_{\vec{k}',\vec{k},\vec{q}_i}|^2 f^0_{\vec{k}}(1-f^0_{\vec{k}'}) n^0_{\vec{q}j} \times \delta(\epsilon_{\vec{k}'} - \epsilon_{\vec{k}} - \hbar\omega_{\vec{q}j}) \delta_{\vec{k}'-\vec{k}-\vec{q}-\vec{Q}_i} . \tag{16}$$

The sum is over the set of reciprocal-lattice vectors $\{\vec{Q}_i\}$. Since the Fermi surface (S_F) of potassium is so very nearly spherical, the $e-p$ coupling should be adequately described by the one-OPW (orthogonalized plane wave) result[40]

$$|g_{\vec{k}',\vec{k},\vec{q}j}|^2 = \hbar(\vec{K}\cdot\vec{e}_{\vec{q}j})^2 V^2(\vec{K})/2MN\omega_{\vec{q}j} . \tag{17}$$

In Eq. (17), $\vec{K} \equiv \vec{k}' - \vec{k}$, $\vec{e}_{\vec{q}j}$ is the polarization vector of the phonon $\vec{q}j$, V is the screened electron-ion pseudopotential form factor for scattering at the S_F, M is the ionic mass and N the number of ions per unit volume. In the term describing the scattering of phonons by entities other than electrons $(r \neq e)$ we have adopted the usual relaxation-time approximation,[38] hence the $\tau^{p-r}_{\vec{q}j}$.

It is important to note that the phonon Boltzmann equation (15) contains a term which depends on the electron deviation from equilibrium function Φ, i.e.,

$$\sum_{\vec{k},\vec{k}'} (\Phi_{\vec{k}} - \Phi_{\vec{k}'}) P^{p-e}_{\vec{k},\vec{q}j;\vec{k}'} . \tag{18}$$

Similarly, the electron Boltzmann equation[38] (which we have not bothered to write down) contains a term depending on the phonon deviation function Ψ. The electron and phonon Boltzmann equations are coupled via these "drag" terms and in principle both equations should be solved simultaneously for Φ and Ψ. However, the phonon drag contribution to the electronic thermal conductivity is always assumed to be unimportant on the grounds[38] that "the flux of phonons, although it may help along the hot $(\epsilon > 0)$ electrons, will hinder their return when cold $(\epsilon < 0)$, and thus has little effect on the total electronic heat current." The drag contribution to the phonon conductivity is similarly dismissed as being very small. Now a key point in the analysis used to extract the phonon conductivity λ^g from the measured magnetothermal resistivity is the assumption that λ^g is independent of B. Since the electron deviation function Φ depends on B, this assumption is only justified to the extent that the drag term can be ignored. For this reason we take a much more detailed look than is usual at the (zero-field) drag effects in potassium. Those willing to accept the usual "hand-waving" arguments may wish to jump ahead to Eq. (23).

It is convenient to write the electron deviation function in the form

$$\Phi_{\vec{k}} \equiv \left(\frac{\nabla T}{T}\right) v_{\vec{k}x} X_{\vec{k}} \equiv \left(\frac{\nabla T}{T}\right) v_{\vec{k}x} \epsilon_{\vec{k}} x_{\vec{k}} , \tag{19}$$

where $\vec{v}_{\vec{k}} \equiv \hbar^{-1}\partial\epsilon_{\vec{k}}/\partial\vec{k}$ is the electron group velocity. In spite of the highly anisotropic nature of the electron-phonon scattering in potassium, the angular variation (over a constant-energy surface) of $x_{\vec{k}}$ has very little effect on the thermal conductivity of even the purest samples.[41,42] (The calculations reported in Refs. 41 and 42 ignored phonon drag. However, for the case of the electrical resistivity phonon drag actually reduces the anisotropy correction[43] and one would expect the same for the electronic thermal resistivity.) On the other hand, the energy dependence of $x_{\vec{k}}$ has a large effect[42,44,45] at the low temperatures $(1.5\ \text{K} \lesssim T \lesssim 4.5\ \text{K})$ of interest here. Hence it should be a good approximation to ignore the small anisotropy correction altogether and write

$$\Phi_{\vec{k}} \cong \left(\frac{\nabla T}{T}\right) v_{\vec{k}x} X(\epsilon_{\vec{k}}) . \tag{20}$$

The electronic thermal conductivity then involves an integration of

$$k^2(\epsilon)v(\epsilon)X(\epsilon)\epsilon(-\partial f^0/\partial\epsilon) \propto (1+3\epsilon/2\mu+\cdots)X(\epsilon)\epsilon \times(-\partial f^0/\partial\epsilon)$$

over all ϵ. Since $\epsilon(-\partial f^0/\partial\epsilon)$ is an odd function of ϵ it is clear that the odd part of $X(\epsilon)$ completely dominates the low-temperature electronic thermal conductivity—the contribution of the even part is many orders of magnitude smaller. Now Leavens[45] has derived a simple one-dimensional integral equation for $X_{\text{odd}}(\epsilon)$ assuming that the phonon-drag contribution is negligible (i.e., setting $\Psi_{\vec{q}j}=0$ in the electron Boltzmann equation). If this derivation is carried out with $\Psi_{\vec{q}j}$ given by Eq. (15) it is not difficult to show that one obtains precisely the same integral equation for $X_{\text{odd}}(\epsilon)$. Thus phonon drag affects the electronic thermal resistivity only through modification of the unimportant even part of $X(\epsilon)$.

We now consider the drag term appearing in the phonon Boltzmann equation. Substituting Eq. (20) into Eq. (18), converting the sums over $\vec{k}$ and $\vec{k}'$ into integrals, and replacing $d\vec{k}$ by $d\epsilon_{\vec{k}}dS_{\vec{k}}/\hbar v_{\vec{k}}$ where $dS_{\vec{k}}\equiv k^2 d\Omega_{\vec{k}}\equiv k^2\sin\theta_{\vec{k}}d\theta_{\vec{k}}d\phi_{\vec{k}}$ is an element of area on the spherical surface of constant energy $\epsilon_{\vec{k}}$ (and similarly for $d\vec{k}'$), Eq. (20) then becomes

$$\left(\frac{\nabla T}{T}\right)\frac{2k_F^4}{(2\pi)^2\hbar^3 v_F}\int_{S_F}d\Omega_{\vec{k}}\int_{S_F}d\Omega_{\vec{k}'}\int_{-\infty}^{+\infty}d\epsilon f^0(\epsilon)[1-f^0(\epsilon+\hbar\omega_{\vec{q}j})] \times[\cos\theta_{\vec{k}}X(\epsilon)-\cos\theta_{\vec{k}'}X(\epsilon+\hbar\omega_{\vec{q}j})]\frac{\hbar n^0_{\vec{q}j}}{2MN\omega_{\vec{q}j}}\sum_t|\vec{K}\cdot\vec{e}_{\vec{q}j}|^2V^2(K)\delta(\vec{K}-\vec{q}-\vec{Q}_t). \tag{21}$$

We have followed the standard procedure[38] of evaluating all slowly varying functions of energy ϵ at the S_F; the corrections to Eq. (21) are negligible, smaller than Eq. (21) by a factor of order k_BT/μ. If we now apply Eqs. (9.10.10) and (9.10.11) of Ref. 38 to the integral over ϵ we obtain

$$-\left(\frac{\nabla T}{T}\right)\frac{k_F^4 n^0_{\vec{q}j}(1+n^0_{\vec{q}j})}{(2\pi)^2\hbar MNv_F}\sum_t\Theta(2k_F-|\vec{q}+\vec{Q}_t|)[(\vec{q}+\vec{Q}_t)\cdot\vec{e}_{\vec{q}j}]^2V^2(\vec{q}+\vec{Q}_t)[\overline{X}_{\text{odd}}(\hbar\omega_{\vec{q}j})I^{(+)}(\vec{q}+\vec{Q}_t)+\overline{X}_{\text{even}}(\hbar\omega_{\vec{q}j})I^{(-)}(\vec{q}+\vec{Q}_t)], \tag{22}$$

where

$$\overline{X}^{\text{even}}_{\text{odd}}(\hbar\omega) \equiv\frac{1}{\hbar\omega}\int_{-\infty}^{\infty}d\epsilon\int_{\epsilon}^{\epsilon+\hbar\omega}d\epsilon' X^{\text{even}}_{\text{odd}}(\epsilon')\left(-\frac{\partial f^0(\epsilon)}{\partial\epsilon}\right)$$

and

$$I^{(\pm)}(\vec{q}+\vec{Q}_t) \equiv\int_{S_F}d\Omega_{\vec{k}}\int_{S_F}d\Omega_{\vec{k}'}(\cos\theta_{\vec{k}'}\pm\cos\theta_{\vec{k}})\delta(\vec{k}-\vec{q}-\vec{Q}_t).$$

The integral $I^{(-)}(\vec{q}+\vec{Q}_t)$ occurs prominently in the theory of the phonon-drag component of the electrical resistivity[41] and is just $2\pi(\vec{q}+\vec{Q}_t)_x/k_F^3|\vec{q}+\vec{Q}_t|$. $I^{(+)}(\vec{q}+\vec{Q}_t)$ is easily shown to be zero. Since the surviving term in Eq. (22) only involves the unimportant even part of $X(\epsilon)$ we conclude that the drag contribution to the phonon conductivity of K is very small. [We have actually checked this by solving the one-dimensional integral equation for $X_{\text{even}}(\epsilon)$ and calculating its contribution to λ^{ϵ}.] The above discussion is directly applicable only to K (and perhaps to Na and Rb as well) because we have assumed a spherical S_F and deviation function of the form Eq. (20). The latter condition can be relaxed to a large extent. The crucial step in the foregoing analysis is the result $I^{(+)}(\vec{q}+\vec{Q}_t)=0$. This result is unchanged if we allow for anisotropy in the $x_{\vec{k}}$ of Eq. (19) by multiplying Eq. (20) by the function

$$\sum_{n=0}^{N}\beta_n\cos^{2n}\theta_{\vec{k}} \quad \text{with } \beta_0=1.$$

(This expression, with $N=2$ and β_1 and β_2 appropriately chosen, accounts very well for the angular dependence of $x_{\vec{k}}$ in potassium.) The corresponding expression for $I^{(\pm)}(\vec{q}+\vec{Q}_t)$ is readily obtained from that given above by replacing $\cos\theta_{\vec{k}'}$, $\pm\cos\theta_{\vec{k}}$ by

$$\sum_{n=0}^{N}\beta_n(\cos^{2n+1}\theta_{\vec{k}'}\pm\cos^{2n+1}\theta_{\vec{k}}).$$

The resulting double surface integral for $I^{(+)}(\vec{q}+\vec{Q}_i)$ is readily shown to be zero [see the Appendix of Ref. 43, where $I^{(-)}(\vec{q}+\vec{Q}_i)$ is evaluated in closed form].

Setting the drag part of Eq. (15) equal to zero and solving for $\Psi_{\vec{q}j}$ we obtain (after various manipulations similar to those outlined above)

$$\Psi_{\vec{q}j}=\left(-\frac{\nabla T}{T}\right)\hbar\omega_{\vec{q}j}u_{\vec{q}jx}\Big/\left[(\tau^{p-e}_{\vec{q}j})^{-1}+\sum_r(\tau^{p-r}_{\vec{q}j})^{-1}\right], \tag{23}$$

where[41]

$$(\tau^{p-e}_{\vec{q}j})^{-1}=\frac{3\pi}{2\hbar v_F^2 k_F M}\sum_i C_j^{(i)}(\vec{q}), \tag{24a}$$

with

$$C_j^{(i)}(\vec{q})\equiv\Theta(2k_F-|\vec{q}+\vec{Q}_i|)\frac{[V(\vec{q}+\vec{Q}_i)(\vec{q}+\vec{Q}_i)\cdot\vec{e}_{\vec{q}j}]^2}{|\vec{q}+\vec{Q}_i|}. \tag{24b}$$

The phonon conductivity,[38] $\lambda^{\mathcal{E}}\equiv -U_x^{\mathcal{E}}/\nabla T$, then follows readily from the expression for the phonon contribution to the thermal current density

$$U_x^{\mathcal{E}}=\frac{1}{(2\pi)^3}\sum_{j=1}^{3}\int_{\mathrm{FBZ}}u_{\vec{q}jx}\hbar\omega_{\vec{q}j}n_{\vec{q}j}\,d\vec{q}.$$

It is

$$\lambda^{\mathcal{E}}=\frac{\hbar^2}{24\pi^3k_BT^2}\sum_{j=1}^{3}\int_{\mathrm{FBZ}}d\vec{q}\,\frac{\omega_{\vec{q}j}^2u_{\vec{q}j}^2n_{\vec{q}j}^0(1+n_{\vec{q}j}^0)}{(\tau^{p-e}_{\vec{q}j})^{-1}+\sum_r(\tau^{p-r}_{\vec{q}j})^{-1}}. \tag{25}$$

It is important to note that $(\tau^{p-e}_{\vec{q}j})^{-1}$ is zero for those phonons for which $(\vec{q}+\vec{Q}_i)\cdot\vec{e}_{\vec{q}j}=0$ for all i allowed by the unit step function Θ, i.e., for transverse phonons with (sufficiently small) wave vectors in the symmetry planes. Hence even if we are in the regime where electrons are, on average, the dominant scatterers of phonons, we cannot completely ignore all other scatterers without getting an infinite phonon conductivity (unless, of course, we go beyond the one-OPW description of K).

Ekin's variational calculation[10] of the phonon conductivity of K explicitly considered just phonon-electron scattering but used as trial function the phonon deviation function appropriate to normal phonon-phonon (p-p) scattering,[38] i.e., $\Psi_{\vec{q}}\propto\vec{q}\cdot\hat{x}$. With this distribution function the collision integral for normal p-p scattering is zero.[38] Hence, in effect, Ekin treated the case of mixed p-e and normal p-p scattering but only in the limit in which the latter completely determines the phonon distribution function (in this limit normal p-p scattering provides no direct contribution to the thermal resistance). Now Kaveh[46] has argued (for the case of the electrical resistivity) that it is just the opposite situation that occurs in K below about 5 K, i.e., p-e scattering dominates and p-p scattering (both normal and umklapp) can be ignored. In this case, Ekin's expression for $\lambda^{\mathcal{E}}$ is not appropriate at the temperatures of interest here ($1.5\ \mathrm{K}\lesssim T\lesssim 4.5\ \mathrm{K}$). Hence it is not surprising that the measured phonon conductivity of K is an order of magnitude larger than that calculated by Ekin.

For temperatures at the lower end of the range of interest we believe that phonon-dislocation (p-d) scattering[47] (or some other scattering mechanism with roughly the same frequency dependence) is the most important mechanism for limiting the mean free path of those troublesome phonons that are scattered only very weakly, or not at all, by the electrons. Of course, the scattering of phonons by other phonons, impurities, grain boundaries, etc., also plays a role. However, in order to make the calculation of $\lambda^{\mathcal{E}}$ tractable and to avoid introducing a large number of unknown parameters characterizing the defect state of a given sample, we concentrate on the most important (in our opinion) scattering mechanisms, i.e., p-e and p-d. In the same spirit we have used Klemens' very simple expression,[48]

$$(\tau^{p-d}_{\vec{q}j})^{-1}=0.605N_Db^2\gamma_G^2\omega_{\vec{q}j},$$

for the p-d scattering rate. N_D is the number of dislocations per cm^2, $\vec{b}$ is the dislocation Burgers vector, and γ_G the Gruneisen constant. Klemens' formula gives only a very rough estimate of the scattering from the strain field of the dislocation and completely ignores any scattering by the dislocation core. Further, we use the relaxation time approximation for the p-d scattering and ignore all mechanisms for equilibrating the phonon distribution function other than p-e and p-d scattering. The adoption of these assumptions means that the dislocation densities obtained in Sec. V by fitting to experiment should not be taken too seriously; they could easily be in error by orders of magnitude. What is important is the actual p-d scattering rate, not the parameter N_D occurring in Klemens' formula. As a further caution, we emphasize the fact that two samples of K with approximately the same residual resisitivity ratio (RRR) can have significantly different dislocation densities because dislocations are not the only defects contributing to the residual resistivity.

As input to the calculation of $\lambda^{\mathcal{E}}$ using Eqs. (23)–(25) we have used the most recent refinement[49] of the first-principles lattice dynamics ($\omega,\vec{e},\vec{u}$) and electron-ion interaction (V) developed originally by Dagens *et al.*[50]

For the range of p-d scattering rates considered ($10^9\ \mathrm{cm}^{-2}\leq N_D\leq 10^{11}\ \mathrm{cm}^{-2}$) and for $T\leq 4$ K the calculated phonon conductivity is proportional to T^2

to within a few percent. Figure 15 shows the calculated λ^g/T^2 as a function of N_D. To give some indication of the relative importance of p-e and p-d scattering we also show λ^g/T^2 calculated with $(\tau^{p-e}_{\vec{q}j})^{-1}$ set equal to zero. For values of N_D representative of the potassium samples actually studied, i.e., $N_D \sim 10^{10}$ cm^{-2}, λ^g/T^2 increases by a factor of ~4 when we switch off the p-e scattering.

The phonon contribution to the zero-field thermoelectric power, i.e., S^g, is obtained most easily by first calculating the Peltier coefficient $\Pi^g_{xx} = -\sigma_{xx} U^g_x / J^e_x$ and then applying the Onsager relation $S^g = \Pi^g_{xx}/T$. Here J_x and U_x are the *isothermal* electric and thermal current densities in the presence of the electric field $\vec{E} = E\hat{x}$. It is clear from Eq. (15) with ∇T set equal to zero that $\Psi_{\vec{q}j}$ and hence S^g would be zero were it not for the drag term. For this reason S^g is referred to as the phonon-drag thermopower. The appropriate expressions for the electron and phonon deviation functions, Φ and Ψ respectively, taking into account the detailed energy dependence but ignoring the less important angular dependence, have been derived by Leavens.[51] The derivation parallels that given above if we replace Eq. (20) by $\Phi_{\vec{k}} \cong eEv_{\vec{k}x}\tau(\epsilon_{\vec{k}})$ and note that for the case of the electrical conductivity it is the even part of τ that is all important.

Opsal[34] has recently used the LAK theory[26] to derive an expression for ϵ''_{yx} in the high-field limit. Using precisely the same microscopic description of potassium as described above we have evaluated Opsal's expression for ϵ^g_{yx}: in our notation

$$\frac{\epsilon^g_{yx}B}{T} = \frac{\hbar c}{16\pi^2 v_F^2 M k_B T^3} \sum_{j=1}^{3} \int_{\mathrm{FBZ}} d\vec{q} \, \frac{\omega_{\vec{q}j} n^0_{\vec{q}j}(1+n^0_{\vec{q}j}) \sum_i C^{(i)}_j(\vec{q})(\vec{q}+\vec{Q}_i)\cdot\vec{u}_{\vec{q}j}}{(\tau^{p-e}_{\vec{q}j})^{-1} + \sum_r (\tau^{p-r}_{\vec{q}j})^{-1}} \, .$$

Figure 16 shows $\epsilon^g_{yx}B/T$ as a function of T calculated in the full phonon drag limit ($N_D = 0$) and also for $N_D = 10^9$, 10^{10}, and 10^{11} cm^{-2}. Clearly p-d scattering has a much less dramatic effect on ϵ^g_{yx} than on λ^g. (For example, at 1 K our calcula-

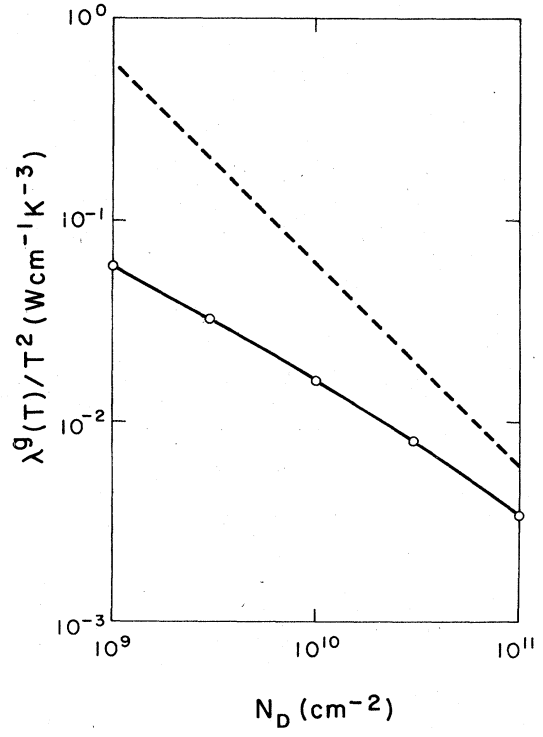

FIG. 15. Calculated variation of λ^g/T^2 as a function of the dislocation density N_D. Dashed line is appropriate to only dislocation scattering of the phonons. Solid line corresponds to scattering of phonons by both dislocations and electrons.

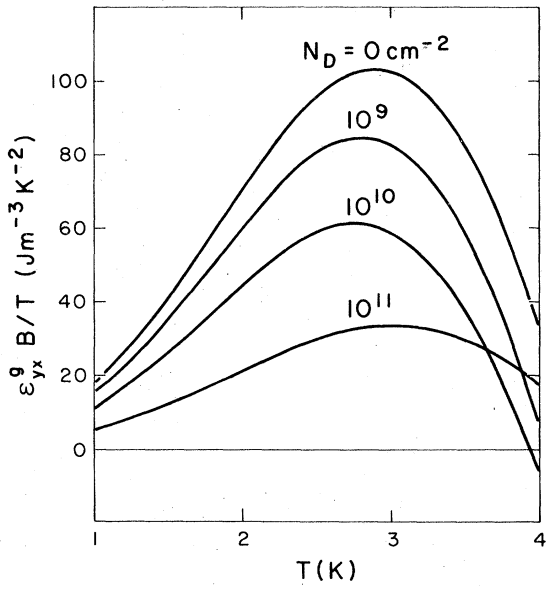

FIG. 16. Calculated phonon-drag contribution to the Nernst-Ettingshausen coefficient, i.e., ϵ^g_{yx} (multiplied by B/T) as a function of temperature for various values of dislocation density N_D. The uppermost curve ($N_D = 0$) is for "full" phonon drag.

tions show that increasing N_D from 10^9 to 10^{10} cm^{-2} decreases ϵ^g_{yx} by 26% but λ^g by 73%.) Nevertheless, the effect of phonon-dislocation scattering is substantial for $N_D \gtrsim 10^9$ cm^{-2}.

In Sec. V, the parameter N_D is determined for each potassium sample by fitting the calculated λ^g shown in Fig. 15 to the very-low-temperature experimental results. Then ϵ^g_{yx} and S^g are computed for this value of N_D and compared with the measured values.

V. COMPARISON OF THEORY AND EXPERIMENT

In this section we interpret the experimental results on samples 2 and 3 (the two for which complete data sets were obtained) in terms of the theory of the preceding section.

Figure 17 shows the measured low-temperature phonon conductivity λ^g as a function of T. Also shown is that calculated assuming mixed p-e and normal p-p scattering with the latter so strong as to completely determine the phonon deviation function Ψ.[10] We have removed the approximation made in Ref. 10 that $\tilde{u}_{\vec{q}j}\cdot\tilde{q} \approx \omega_{\vec{q}j}$. This approximation is a good one at very low temperatures ($T \lesssim 2$ K) but breaks down quite badly at high temperatures. The calculated λ^g is an order of magnitude smaller than what is observed. Moreover, this poor agreement between theory and experiment cannot be improved without relaxing the assumption on Ψ; just adding further mechanisms for scattering the phonons can only lower the calculated λ^g, thus increasing the discrepancy. At the other extreme, we can calculate λ^g completely ignoring p-p scattering. The results obtained using Eq. (25) for the case of mixed p-e and p-d scattering are also shown in Fig. 17. For each sample the strength of the p-d scattering has been adjusted (using Fig. 15) so that theory and experiment agree at the lowest temperature (about 1.5 K). Theory and experiment coincide until about 2.5 K, above which temperature the experimental results fall increasingly below the theoretical curve (which varies as T^2 to within a few percent). This behavior can be interpreted quite readily as indicating the onset of significant p-p or possibly phonon–impurity (isotope) scattering at about 2.5 K. (Brian Pippard and Manfred Jericho pointed out the possible importance of the latter.) Unfortunately, inclusion of p-p scattering in our calculations appears to be an intractable problem at the present time. For this reason, it is highly desirable to test our interpretation of the T dependence of the measured phonon conductivity by comparing theory (with no further adjustment of parameters) and experiment for some other property which is sensitive to phonon scattering. The off-diagonal component ϵ''_{yx} of the high-field thermoelectric tensor is ideal for this purpose.

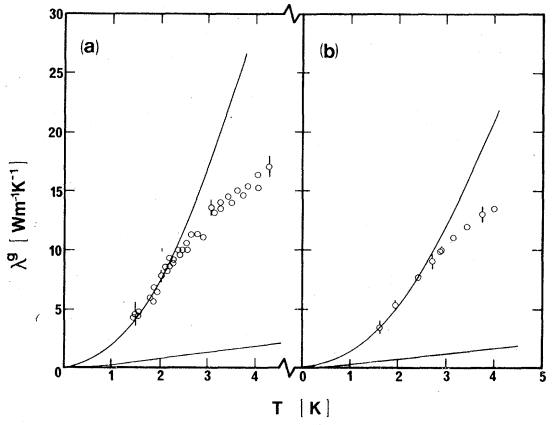

FIG. 17. Theoretical fits to the lattice thermal conductivity: (a) The data on sample 2 fitted with $N_D = 8\times10^9$ cm^{-2}. (b) The data on sample 3 (third series), i.e., after warming to room temperature twice fitted with $N_D = 1.4\times10^{10}$ cm^{-2}. In both cases the lower curve is calculated assuming phonon-phonon scattering is predominant (see text) while the curves through the data are calculated assuming phonon-phonon scattering can be ignored.

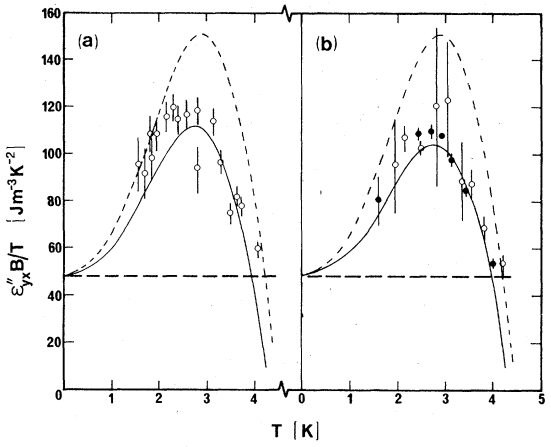

FIG. 18. Calculated variation of $\epsilon''_{yx}B/T$ for samples 2 and 3. Horizontal heavy dashed line is the diffusion component $\epsilon^d_{yx}B/T$. Thin dashed curves show the calculated variation of $\epsilon''_{yx}B/T$ appropriate to full phonon drag ($N_D = 0$). For sample 2, (a) the solid line is calculated using $N_D = 8\times10^9$ cm^{-2} and for sample 3, (b) the solid line uses $N_D = 1.4\times10^{10}$ cm^{-2} (see Fig. 17). Solid circles for sample 3 represent our most accurate data on any sample.

Figure 18 shows theoretical and experimental results for $\epsilon''_{yx}B/T$ in the high-field limit. The horizontal dashed line is $\epsilon^d_{yx}B/T = \gamma$ with the electronic specific-heat ($C^e = \gamma T$) coefficient taken directly from experiment.[33] If phonon drag were absent (i.e., completely quenched) in the samples

under consideration then the experimental results should coincide with this line. That they do not indicates directly and unambiguously the presence of significant phonon drag. To our knowledge, no other experiment gives such a clear-cut demonstration of the presence of substantial phonon drag in K. The theoretical curve labeled $N_D = 0$ shows the full phonon-drag (or zero-quenching) case and was calculated assuming that the phonons are scattered only by electrons. This calculation is quite insensitive below $T \approx 3.5$ K (i.e., well below the region of almost complete cancellation of the normal and umklapp p-e scattering contributions to ϵ_{yx}^{g}) to the choice of lattice dynamics and pseudopotential form factor. [This is in marked contrast to the ideal electrical resistivity, which is extremely sensitive to the choice of input, particularly the pseudopotential form factor $V(K)$ at $K = 2k_F$.] Comparison of the experimental results with the calculated zero-quenching curve in the region $T \lesssim 3.5$ K thus demonstrates very clearly that, whatever the mechanism, phonon drag is quenched to a significant extent in samples 2 and 3.

The above discussion of ϵ_{yx}^{g} makes no reference to our work on λ^{g}. To make contact we also show, for each of the samples 2 and 3, $\epsilon_{yx}'' B/T$ calculated with exactly the same p-d scattering rate that was obtained by fitting to λ^{g}. The good agreement between theory and experiment provides strong support of our interpretation of the temperature dependence of λ^{g}. ϵ_{yx}'' is much less sensitive than λ^{g} to any mechanism for scattering those phonons which are very weakly scattered by electrons. Hence it comes as no surprise that the onset of significant p-p scattering is delayed to a higher temperature (≈ 3.5 K for ϵ_{yx}'' as compared to ≈ 2.5 K for λ^{g}). It is of interest to note that the group of phonons most effective in contributing to λ^{g} is the least effective in producing ϵ_{yx}^{g}. This arises simply because, other things being equal, it is those phonons that are least scattered by the electrons that are most effective in carrying the heat current in the presence of a temperature gradient; on the other hand, in the presence of an electric field they are dragged along the least by the current of electrons and thus make little contribution to the phonon-drag component of ϵ_{yx}, i.e., ϵ_{yx}^{g}. The two properties λ^{g} and ϵ_{yx}^{g} thus tend to sample different phonons with different weights. Thus the fact that using the same p-d scattering rate in both calculations leads to simultaneous good agreement with experiment is a very satisfactory result.

Finally we turn to the zero-field thermopower. We have calculated S^{g} using exactly the same input as previously, i.e., for no p-d scattering and for the p-d scattering rate fit to the low-temperature phonon conductivity. The detailed energy dependence of the electronic "relaxation time" τ, a complication that does not arise in the high-field limit of ϵ_{yx}^{g}, was included in the calculation by numerically solving the coupled electron and phonon Boltzmann equations[51]; this is important in the region where there is a very large cancellation between the normal and umklapp p-e contributions to S^{g}, but has only a tiny effect on the position and height of the calculated negative peak in S^{g}. Consequently, the inclusion of the angular dependence of τ, which is known to be less important than the energy dependence in calculating the thermal and electrical resistivities of K, is most unlikely to modify our conclusions.

The only remaining problem is to allow for the diffusion contribution S^{d}. At the very low temperatures of interest here ($T/\Theta_D \lesssim 0.05$) the various Nielsen-Taylor[13] and Hasegawa[14] contributions to S^{d} are essentially linear in T. Hence even if we include these complications as well as the many-body renormalization effects, discussed by Opsal *et al.*,[12] Lyo,[12] and Vilenkin and Taylor,[52] we expect S^{d} to be approximately linear in T. (Accidental cancellation of all linear contributions could lead to a more complex T dependence but the amplitude would be very small relative to the observed negative peak in S.) Thus the theoretical curves of Fig. 19 were constructed by assuming $S = \delta T + S^{g}$, with S^{g} the calculated values and δ chosen by fitting this expression to the experimental

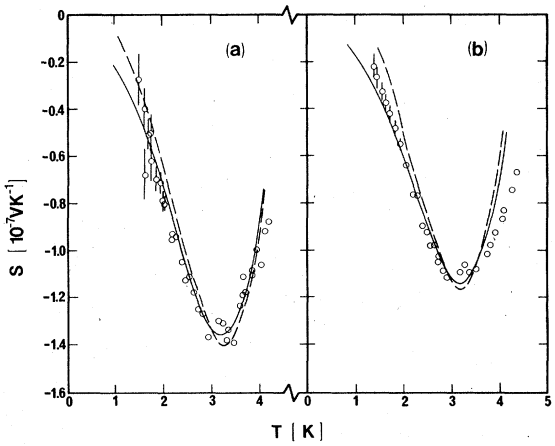

FIG. 19. Measured and calculated zero-field thermopowers S of samples 2 and 3 using $S = \delta T + S^{g}$, where δ is adjusted for best fit. Dashed lines are the best fits using full phonon drag (i.e., $N_D = 0$); for sample 2 (a) this yields $\delta = +0.15 \times 10^{-7}$ V K^{-2} and for sample 3 (b) $\delta = +0.09 \times 10^{-7}$ VK^{-2}. Full lines are the best fits using the same values of N_D as were appropriate to Fig. 17 and 18 (i.e., $N_D = 8 \times 10^{9}$ cm^{-2} for sample 2, $N_D = 1.4 \times 10^{10}$ cm^{-2} for sample 3) and give $\delta = -0.16 \times 10^{-7}$ V K^{-2} for sample 2 and $\delta = -0.12 \times 10^{-7}$ V K^{-2} for sample 3.

results. For the broken curves S^g was calculated assuming no p-d scattering; for each of the solid curves the p-d scattering rate obtained by fitting to λ^g was included in the calculation. It is clear from the figure that for both samples 2 and 3 there is little to choose between the solid and dashed curve, each giving a good representation of the experimental data. One might be inclined to prefer the curves for the quenched-phonon-drag case because the fitted values of δ, -0.161×10^{-7} V K^{-2} (sample 2) and -0.116×10^{-7} V K^{-2} (sample 3), are not very different from the well-known result $\delta = -\pi^2 k_B^2/3|e|\mu = -0.116\times10^{7}$ V K^{-2} that one obtains for free electrons scattered by hard spheres. However, the fitted values of δ for the full-phonon-drag case (no p-d scattering), $+0.015\times10^{-7}$ V K^{-2} (sample 2) and $+0.090\times10^{-7}$ V K^{-2} V K^{-2} (sample 3), cannot be ruled out because of the complications referred to above. It is necessary to do an accurate first-principles calculation of S^d, including all the relevant features of the electronic scattering as well as the mass and velocity renormalizations, in order to pin down the correct value of δ for a given sample. This could very well require quite detailed knowledge of the defect state of the sample. Moreover, one would probably find that the low-temperature electron-diffusion thermopower S^d is only approximately linear in T.

The above emphasizes the importance of measurements of ϵ''_{yx} in the high-field limit where one knows from theory that $\epsilon^d_{yx}B$ is rigorously equal to the electronic specific heat which is accurately known experimentally. Hence there is no ambiguity in extracting the phonon-drag contribution from the measured ϵ''_{yx}.

VI. SUMMARY

The main conclusion to be drawn from this work is that the thermomagnetic and thermoelectric properties of potassium can be understood remarkably well with so few assumptions. The unusual behavior of the transverse and Righi-Leduc thermal resistivities is due solely to the presence of a large lattice thermal conductivity with an unusual temperature dependence. In retrospect this high lattice conductivity should have been expected (and indeed was by some authors[53]) as a result of the free-electron-like character of potassium. Detailed calculations support the experimental results. We infer that, because certain transverse phonons are so very weakly scattered by the electrons, other scattering mechanisms must be responsible for finally limiting their mean free paths and preventing the extremely high phonon conductivity that would otherwise occur. It is suggested that, over the experimental range (1.5 K$\lesssim T\lesssim$ 4 K), phonon-dislocation scattering (or some other scattering mechanism with a similar dependence on phonon frequency) is most effective in this regard and calculations have been presented to support this view. Above about 2.5 K the measured phonon conductivity falls increasingly below the T^2 behavior that is observed at lower temperatures and also predicted (but to a much higher temperature) for the case of mixed phonon-electron and phonon-dislocation scattering; this departure presumably signifies the onset of significant phonon-phonon scattering, or possibly phonon–impurity (isotope) scattering.

Observations and calculations have also been made on the high-field Nernst-Ettingshausen coefficient. The analysis provides not only a direct and unambiguous quantitative demonstration of a significant phonon-drag effect in potassium, but also a good estimate of the amount by which it has been quenched from the full phonon-drag limit. (The corresponding analysis for the case of the zero-field thermopower is not nearly so clear cut and reliable because the electron-diffusion component is not accurately known either theoretically or experimentally.) Finally we have shown that the same strength of phonon-dislocation scattering that was required to give good agreement with the low-temperature phonon conductivity also provides the correct amount of quenching of the phonon drag in the Nernst-Ettingshausen coefficient.

Note added in proof. A recent paper [P. J. Tausch, R. S. Newrock, and W. Mitchel, Phys. Rev. B 20, 501, (1979)] deals with the high-field transverse thermal magnetoresistance of K. The data presented in this paper, and relevant to the present study, are the same as those discussed in the papers in Ref. 7; all our comments concerning those papers are equally applicable to this most recent paper.

APPENDIX: END EFFECTS IN HIGH MAGNETIC FIELDS

Lippmann and Kuhrt[54] and more recently Sampsell and Garland[18] have shown that the nature of the current contacts can lead to anomalous behavior in the measurement of the magnetoresistance of rectangular plates. However, these end effects are not present[55] under the usual experimental conditions for which voltage probes are recessed in from the ends of the sample.

We consider a homogeneous rectangular plate of length l, width w, and thickness t having resistivity elements ρ_{xx} and ρ_{yx} when a magnetic field $B\hat{z}$ is present. Current enters or leaves the sample through the equipotential surfaces along $y=0$ and $y=l$. Voltage probes are located a distance c from each end of the sample (on the $x=w$

edge) and are assumed not to disturb the current flow lines. Then for a total current I through the sample, the component of electric field parallel to $\hat{y}$, E_y, along the edge $x=w$, is given by Jensen and Smith[55] as (taking $\rho_{yy}=\rho_{xx}$)

$$E_y(y)=(\rho_{xx}I/wt)\left(\frac{\zeta(y/w)-1}{\zeta(y/w)+1}\right)^{\theta/\pi}\left(\frac{1+k\zeta(y/w)}{1-k\zeta(y/w)}\right)^{\theta/\pi}. \tag{A1}$$

Here θ is the Hall angle ($\tan\theta=\rho_{yx}/\rho_{xx}$), the function ζ is defined by

$$\frac{y}{w}=\left(\frac{1}{\pi}\right)\int_1^{\zeta}(\xi^2-1)^{-1/2}(1-k^2\xi^2)^{-1/2}\,d\xi \tag{A2}$$

and the parameter k is given (for $l/w\gtrsim 2$) by

$$k=4\exp(-\pi l/w). \tag{A3}$$

For a very long sample ($l/w\to\infty$), with $c\gg w$, the current between the voltage probes flows nearly parallel to the y direction. In this limit the field E_y is constant and Eq. (A1) reduces to the equation usually applied in calculations of ρ_{xx},

$$E_y=\rho_{xx}I/wt, \quad l/w\to\infty. \tag{A4}$$

In practice, a voltage V is measured between the probes, which will be given by

$$V=\int_c^{l-c}E_y(y)\,dy. \tag{A5}$$

Then, in light of (A4) and (A5), the true ρ_{xx} will not be obtained if l/w is finite; rather an effective resistivity ρ_{eff} would be calculated as

$$\rho_{\text{eff}}=\frac{wt}{I(l-2c)}\int_c^{l-c}E_y(y)\,dy. \tag{A6}$$

This effective resistivity is dependent upon the ratio l/w, the amount c by which the voltage probes are inset, and the Hall angle θ. Using (A1) we obtain

$$\frac{\rho_{\text{eff}}}{\rho_{xx}}=\frac{1}{l-2c}\int_c^{l-c}\left(\frac{\zeta(y/w)-1}{\zeta(y/w)+1}\right)^{\theta/\pi}\left(\frac{1+k\zeta(y/w)}{1-k\zeta(y/w)}\right)^{\theta/\pi}dy. \tag{A7}$$

This expression has been evaluated numerically under a variety of conditions; in particular we consider a free-electron model so that $\tan\theta=\omega\tau$, where ω is the cyclotron frequency and τ is the relaxation time. The linear magnetoresistance obtained by Lippmann and Kuhrt[54] is obtained only in the limit $c\to 0$. When c is nonzero (as is the case in four-probe measurements) ρ_{eff} saturates in high magnetic fields; and for $l/w>5$ and $c/w>1$, ρ_{eff} and ρ_{xx} will be the same to better than 0.1%. For the potassium samples actually used in this study, these quantities were the same to within 0.02%. Similar arguments apply to γ_{xx}.

[1]R. Fletcher, Phys. Rev. Lett. 32, 930 (1974).
[2]R. Fletcher, J. Phys. F 4, 1155 (1974).
[3]Throughout this paper we adopt the traditional viewpoint that potassium is a cubic very nearly-free-electron metal. For a review of the evidence in favor of the contrary point of view, see A. W. Overhauser, Adv. Phys. 27, 243 (1978).
[4]M. Ia Azbel', M. I. Kaganov, and I. M. Lifshitz, Zh. Eksp. Teor. Fiz. 32, 1188 (1957) [Sov. Phys.-JETP 5, 967 (1957)].
[5]R. S. Newrock and B. W. Maxfield, Solid State Commun. 13, 927 (1973).
[6]R. S. Newrock and B. W. Maxfield, J. Low Temp. Phys. 23, 119 (1976).
[7]P. J. Tausch and R. S. Newrock, Phys. Rev. B 16, 5381 (1977); Commun. Phys. 2, 187 (1977).
[8]R. Fletcher and M. R. Stinson, J. Phys. (Paris) 39(C-6), 1028 (1978); R. Fletcher and J. L. Opsal, Phys. Rev. B 20, 2555 (1979).
[9]T. Amundsen, Philos. Mag. 20, 687 (1969); C. H. Stephan and B. W. Maxfield, Solid State Commun. 7, 1039 (1969); B. J. Thaler and R. Fletcher, J. Low Temp. Phys. 30, 773 (1978).
[10]J. W. Ekin, Phys. Rev. B 6, 371 (1972).
[11]R. J. Douglas and R. Fletcher, Philos. Mag. 32, 73 (1974).
[12]J. L. Opsal, B. J. Thaler, and J. Bass, Phys. Rev. Lett. 36, 1211 (1976); S. K. Lyo, Phys. Rev. B 17, 2545 (1978); B. J. Thaler, R. Fletcher, and J. Bass, J. Phys. F 8, 131 (1978).
[13]P. E. Nielsen and P. L. Taylor, Phys. Rev. B 10, 4061 (1974).
[14]A. Hasegawa, Solid State Commun. 15, 1361 (1974); J. Phys. F 4, 2164 (1974).
[15]M. R. Stinson, R. Fletcher, and C. R. Leavens, J. Phys. F 9, L107 (1979).
[16]Mine Safety Appliances Ltd., Callery, PA.
[17]R. Fletcher and A. J. Friedman, Phys. Rev. B 8, 5381 (1973).
[18]See, e.g., J. B. Sampsell and J. C. Garland, AIP Conf. Proc. 40, 395 (1978) [Conference on the Electrical Transport and Optical Properties of Inhomogeneous Media, Columbus, Ohio (1977)].
[19]R. Fletcher, J. Low Temp. Phys. 22, 39 (1976); Phys. Rev. B 14, 4329 (1976).
[20]R. Fletcher, Cryogenics 17, 529 (1977).
[21]G. J. Edwards, J. Phys. E 4, 299 (1971).
[22]Emerson and Cuming, Inc., Canton, MA.
[23]R. Fletcher and M. R. Stinson, J. Phys. E 12, 92 (1979).
[24]S. A. Werner, E. Gurmen, and A. Arrott, Phys. Rev. 186, 705 (1969).
[25]H. Taub, Phys. Condens. Matter 19, 107 (1975).
[26]I. M. Lifshitz, M. Ia. Azbel', and M. I. Kaganov, Zh. Eksp. Teor. Fiz. 31, 63 (1956) [Sov. Phys.-JETP 4, 41 (1957)].

[27]R. Fletcher and M. R. Stinson, J. Low Temp. Phys. 27, 787 (1977).
[28]H. N. De Lang, H. van Kempen, and P. Wyder, J. Phys. F 8, L39 (1978); H. van Kempen, H. N. De Lang, J. S. Lass, and P. Wyder, Phys. Lett. A 42, 277 (1972).
[29]E. P. Esposito, R. S. Newrock, and K. Loeffler, Phys. Rev. Lett. 41, 818 (1978).
[30]Measurements on λ_0 have previously been published by R. S. Newrock and B. W. Maxfield, Phys. Rev. B 7, 1283 (1973).
[31]D. K. Wagner, Phys. Rev. B 5, 336 (1972).
[32]R. Fletcher, Phys. Rev. B 15, 3602 (1977).
[33]N. E. Phillips, Crit. Rev. Solid State Sci. 2, 467 (1971).
[34]J. L. Opsal, J. Phys. F 7, 2349 (1977).
[35]D. K. C. MacDonald, W. B. Pearson, and I. M. Templeton, Philos. Mag. 3, 917 (1958); Proc. R. Soc. London A 248, 107 (1958).
[36]F. J. Blatt, P. A. Schroeder, C. L. Foiles, and D. Greig, *Thermoelectric Power of Metals* (Plenum, New York, 1976).
[37]B. J. Thaler and R. Fletcher, J. Low Temp. Phys. 30, 773 (1978).
[38]J. M. Ziman, *Electrons and Phonons* (Oxford University, London, 1960).
[39]M. Bailyn, Phys. Rev. 112, 1587 (1958).
[40]L. J. Sham and J. M. Ziman, *Solid State Physics* (Academic, New York, 1963), Vol. 15.
[41]F. W. Kus, J. Phys. F 6, 59 (1976).
[42]W. D. Jumper and W. E. Lawrence, Phys. Rev. B 16, 3314 (1977).
[43]C. R. Leavens and M. J. Laubitz, J. Phys. F 6, 1851 (1976).
[44]P. G. Klemens, Aust. J. Phys. 7, 64 (1954).
[45]C. R. Leavens, J. Phys. F 7, 163 (1977).
[46]M. Kaveh, Phys. Rev. B 15, 3788 (1977).
[47]R. Taylor, C. R. Leavens, M. S. Duesbury, and M. J. Laubitz, J. Phys. (Paris) 39(C-6), 1058 (1978).
[48]P. G. Klemens, *Thermal Conductivity* (Academic, New York, 1969).
[49]C. R. Leavens and R. Taylor, J. Phys. F 8, 1969 (1978).
[50]L. Dagens, M. Rasolt, and R. Taylor, Phys. Rev. B 11, 2726 (1975).
[51]C. R. Leavens, J. Phys. F 7, 1297 (1977).
[52]A. Vilenkin and P. L. Taylor, Bull. Am. Phys. Soc. 23, 428 (1978).
[53]M. A. Archibald, J. E. Dunick, and M. H. Jericho, Phys. Rev. 153, 786 (1967).
[54]H. J. Lippmann and R. Kuhrt, Z. Naturforsch. 13, 462 (1958).
[55]H. H. Jensen and H. Smith, J. Phys. C 5, 2867 (1972).